The fine-structural distribution of G-protein receptor kinase 3, β-arrestin-2, Ca2+/calmodulin-dependent protein kinase II and phosphodiesterase PDE1C2, and a Cl−-cotransporter in...

ARTICLE *in* JOURNAL OF NEUROCYTOLOGY · APRIL 2005

Impact Factor: 1.94 · DOI: 10.1007/s11068-005-5045-9 · Source: PubMed

1 AUTHOR:

Bert Ph M Menco
Northwestern University
66 PUBLICATIONS **2,894** CITATIONS

SEE PROFILE

Journal of Neurocytology **34**, 11–36 (2005)

The fine-structural distribution of G-protein receptor kinase 3, β-arrestin-2, Ca^{2+}/calmodulin-dependent protein kinase II and phosphodiesterase PDE1C2, and a Cl^--cotransporter in rodent olfactory epithelia

BERT PH. M. MENCO*

Department of Neurobiology & Physiology, O. T. Hogan Hall, Northwestern University, 2205 Tech Drive, Evanston, IL 60208-3520
bertmenco@northwestern.edu

Received 11 November 2005; revised 25 February 2005; accepted 25 February 2005

Abstract

The sequentially activated molecules of olfactory signal-onset are mostly concentrated in the long, thin distal parts of olfactory epithelial receptor cell cilia. Is this also true for molecules of olfactory signal-termination and -regulation? G-protein receptor kinase 3 (GRK3) supposedly aids in signal desensitization at the level of odor receptors, whereas β-arrestin-2, Ca^{2+}/calmodulin-dependent protein kinase II (CaMKII) and phosphodiesterase (PDE) PDE1C2 are thought to do so at the level of the adenylyl cyclase, ACIII. The Na^+, K^+-$2Cl^-$-cotransporter NKCC1 regulates Cl^--channel activity. In an attempt to localize the subcellular sites olfactory signal-termination and -regulation we used four antibodies to GRK3, two to β-arrestin-2, five to CaMKII (one to both the α and β form, and two each specific to CaMKII α and β), two to PDE1C2, and three to Cl^--cotransporters. Only antibodies to Cl^--cotransporters labeled cytoplasmic compartments of, especially, supporting cells but also those of receptor cells. For all other antibodies, immunoreactivity was mostly restricted to the olfactory epithelial luminal border, confirming light microscopic studies that had shown that antibodies to GRK3, β- arrestin-2, CaMKII, and PDE1C2 labeled this region. Labeling did indeed include receptor cell cilia but occurred in microvilli of neighboring supporting cells as well. Apical parts of microvillous cells that are distinct from supporting cells, and also of ciliated respiratory cells, immunoreacted slightly with most antibodies. When peptides were available, antibody preabsorption with an excess of peptide reduced labeling intensities. Though some of the antibodies did label apices and microvilli of vomeronasal (VNO) supporting cells, none immunoreacted with VNO sensory structures.

Introduction

Biochemistry, physiology and light microscopy inquests have provided significant insight in the termination and regulation of olfactory signal-onset (some reviews: Frings, 2001; Kini & Firestein, 2001; Moon & Ronnett, 2003; Nakamura, 2000). However, apart from one study (Asanuma & Nomura, 1993), the fine structural location of any of the molecules reportedly involved in these parts of the olfactory signaling cascade was lacking. This study serves to partly fill that gap. Earlier works showed that key molecules of olfactory signal-onset occur primarily in specialized distal parts of receptor cell cilia, the subcellular structures that are most likely to interact with incoming odor molecules (reviewed in Menco, 1997; Menco & Morrison, 2003; see also Kulaga *et al*., 2004; Schwarzenbacher *et al*., 2005; Strotmann *et al*., 2004). Here we tested whether anticipated molecules of olfactory signal-termination and -regulation are present in the same subcellular compartments. For example, G-protein-coupled receptor kinase 3 (GRK3, also called β-ARK2; Boekhoff *et al*., 1994; Bruch *et al*., 1997; Dawson *et al*., 1993; Peppel *et al*., 1997; Schleicher *et al*., 1993) and Ca^{2+}/calmodulin-dependent protein kinase II (CaMKII; Wei *et al*., 1998) are important candidate molecules to mediate olfactory signal termination (review, Zufall & Leinders-Zufall, 2000). GRK3 is thought to act at the level of odor receptors, while CaMKII acts at the level of a special adenylyl cyclase involved in olfactory signaling, Type 3 (ACIII; for a flow diagram, see, e.g., Fig. 4 in Nakamura, 2000). Earlier light-microscopic studies demonstrated immunoreactivity for these molecules in the olfactory epithelial border

* To whom correspondence should be addressed.

that contains the receptor cell cilia (Dawson *et al*., 1993; Wei *et al*., 1998). The same was true for some other molecules of signal termination, β-arrestin-2 (Dawson *et al*., 1993) and the Ca^{2+}/calmodulin-dependent phosphodiesterase (PDE) PDE1C2 (Juilfs *et al*., 1997; see also Borisy *et al*., 1992). The Na^+, K^+-$2Cl^-$-cotransporter NKCC1 plays an important role in Cl^-- homeostasis, also in the olfactory epithelium (Kaneko *et al*., 2004), where it maintains the Cl^--concentration above electrochemical equilibrium (Reisert *et al*., 2005; Restrepo, 2005). With light microscopy NKCC1 is mainly found in receptor cell dendrites and cell bodies rather then cilia (Reisert *et al*., 2005; see also legend Table 1). The fine-structural localization of this important molecule was also included here.

It was not completely clear for any of the listed molecules whether the labeling in the epithelial surface, as seen with light-microscopy, pertains only to receptor cell cilia, and perhaps dendritic endings, or whether apical parts of neighboring cells, in particular microvilli of supporting cells, also labeled. Therefore, a more accurate assessment establishing the fine-structural localization of these molecules is essential. Indeed, the present work validates the light-microscopic studies in that the olfactory epithelial border that contains the cilia of the receptor cells is immunoreactive for all molecules mentioned above. However, the data demonstrates that the labeling patterns are more complex. Some of the results of this work was presented before in abstract form (Menco, 2004).

Materials and methods

ANIMAL SELECTION

Young adult Sprague-Dawley rats and Swiss Webster mice (Harlan, Indianapolis, Indiana) were used for electron microscopy, about 10 animals total. All procedures described below were performed in accordance with Federal and NIH animal-use guidelines, using institution-approved animal protocols.

TISSUE PREPARATION AND FREEZE-SUBSTITUTION

Sections were taken from the same animals and tissues as those prepared for earlier studies (Menco *et al*., 1997, 2001). Therefore, tissue collection and preparation is described only briefly below. Once resin-embedded, immunoreactivity is preserved for several years (Menco, 1995). For example, in a recent study we showed that the fine-structural immunoreactivity of olfactory receptor cells for olfactory marker protein (OMP) remained prominent in such blocks (e.g., Koo *et al*., 2004, and unpublished). The restricted use of animals is one advantage of post-embedding immunocytochemistry. In addition, antibodies can access potential antigens throughout the tissue sections, and expensive antibodies can be recycled to be used again.

Some rats and mice were asphyxiated with CO_2. Nasal tissues from these animals were, without further chemical fixation, rapidly frozen by dropping them on a liquid nitrogen-cooled copper block (Unfix, Column B in Table 1; Gentleman Jim Quick-Freeze System: Energy Beam Sciences, Agawam, Massachusetts; Phillips & Boyne, 1984). Others were deeply anesthetized with 85 mg/kg sodium pentobarbital, injected intraperitoneally, and transcardially perfusion-fixed with 4% freshly depolymerized paraformaldehyde (Para, Column B in Table 1) or 4% freshly depolymerized paraformaldehyde supplemented with 0.1% glutaraldehyde (Glu, Column B in Table 1) in 0.1 M Sorensen phosphate buffer (pH 7.2) + 0.15 mM $CaCl_2$. Following these procedures, the nasal septa (and sometimes turbinates) covered with olfactory epithelium and vomeronasal tissues were excised for further processing. The excised tissues were further fixed, cryoprotected (essentially according to methods developed by Van Lookeren Campagne *et al.* (1991)), and rapidly frozen by dropping them in liquid propane using the Gentleman Jim Quick-Freezing System. All specimens were freeze-substituted and embedded as described in Menco *et al*. (1997, 2001). The unfixed specimens were freeze-substituted in dry acetone/0.1% uranyl acetate (UAc); fixed specimens were freeze-substituted in methanol /0.1% UAc. Freeze-substitution, infiltration, and low-temperature embedding were carried out in a CS Auto Cryo-Substitution System (Leica, Vienna, Austria). Infiltrated specimens were embedded in Lowicryl K11M (Chemische Werke Lowi G.m.b.H., Waldkraiburg, Germany) while the temperature rose slowly from -60°C to ambient. The whole procedure lasted about one month.

ANTIBODIES

With the exception of those to the phosphodiesterase PDE1C2, one of the antibodies to β-arrestin-2, those to NKCC1/2 and KCC2, and the controls (OMP, $G_{olf\alpha}$ and 1F4), the antibodies were obtained from commercial sources. Details regarding such pertinent information as antibody sources, referring literature, and dilutions are presented in Table 1 and its legend.

IMMUNOCYTOCHEMISTRY

150–200 nm thick sections, were cut with a Leica Ultramicrotome S. Immunocytochemistry was carried out as described earlier (Menco *et al*., 1997, 2001). In short: Tris-buffered saline, 0.01 M, pH 8.0, supplemented with 0.5 M NaCl, 0.1% acetylated BSA (AcBSA, Aurion, Electron Microscopy Sciences, Fort Washington, PA) and 0.05% sodium azide (TBS/AcBSA), was used for blocking, incubations, dilutions, and most washings. Sections were immersed in the blocking solution for three to four hours at room temperature. Subsequently, they were incubated with primary antibodies at appropriate dilutions (Table 1 and figure legends) in the same solution overnight at 4°C. Depending on the animal in which the primary antibodies were raised, antibody binding was visualized with goat-anti-rabbit IgG (GAR), goat-anti-rabbit GAR-F(ab')2-fragments (GAR-FAB), rabbit-anti-goat IgG (RAG), goat-anti-mouse IgG, or protein G (Pr G) as secondary probes. All of these probes were presented conjugated to 15-nm gold particles (Aurion) with an OD_{520} (optical density at 520 nm) of about 0.07–0.08. Gold conjugates were diluted with the same buffer in which they were supplied, supplemented with 0.1% AcBSA. The sections were exposed to these gold probes for about 4 hours at room temperature. The blocking buffer was supplemented with 0.1% Tween 20 for the one-minute jet-washing that followed the gold incubation. Next, the grids were jet-washed with distilled water for one minute.

Table 1. A summary of tissues, fixation conditions, antibodies and their dilutions and secondary probes that were conjugated to 15-nm colloidal gold.

A Species	B Fixation condition	C Antibody to	D Tissue	E Antibody source	F Antibody code	G Antibody dilutions and special conditions	H Peptide excess (w/w) for blocking	I Secondary probe[1]
1. Rat, Mouse[2]	**Fix-para[3], Fix-glu[3], Unfix**	**GRK3[3]**	**Olf**	**Santa Cruz, Santa Cruz, CA**	**SC-9306 (E-15, C[3])**	**Und[3]-1/1000, Tw[3], Bl Prot[3] x200, ap[3]**	**x10-x100**	**RAG**
2. Rat, Mouse	**Fix-para, Fix-glu, Unfix**	**GRK3**	**Olf**	**Santa Cruz**	**SC-563 (C-14, C)**	**Und-1/1000, Tw, Bl Prot x100, ap**	**x5**	**GAR**
3. Rat, Mouse	Fix-para, Fix-glu, Unfix	GRK2/3	Olf	Sigma, St. Louis, MO	G4665 (467-688, C)	Und-1/350, Tw, ap		GAM
4. Rat, Mouse	**Fix-para, Unfix**	**GRK2/3**	**Olf, VNO**	**Upstate, Lake Placid, NY; Dawson *et al.*, 1993**	**05-465 (467-688, C)[4]**	**1/5-1/1000, ap**		**GAM**
5. Rat	**Fix-para, Unfix**	**β-Arrestin-2**	**Olf**	**Santa Cruz**	**SC-13140 (H-9, 1-250, N)**	**Und-1/100, Bl Prot x100, ap**	**x5**	**GAM**
6. Rat, Mouse	**Fix-para, Unfix**	**β-Arrestin-2**	**Olf, VNO**	**R. J. Lefkowitz, Duke University; Dawson *et al.*, 1993**	**A2CT/7435-3 (336-411, C)[4]**	**1/5—1/25, ap**		**GAR**
7. Rat, Mouse	**Fix-para, Fix-glu, Unfix**	**CaMKIIα/β[3]**	**Olf, VNO**	**Santa Cruz**	**SC-9035 (M-176, 303-478, C)**	**Und-1/100, Tw, ap**		**GAR**
8. Rat	Fix-para, Unfix	CaMKII α	Olf	Santa Cruz	SC-5391 (L-15, int)	1/10—1/1000, ap		RAG
9. Rat	Fix-para, Unfix	CaMKII β	Olf	Santa Cruz	SC-1540 (C-20, C)	1/10—1/1000, ap		RAG
10. Rat	Fix-para, Unfix	CaMKII α	Olf VNO	Zymed, San Francisco, CA; Wei *et al.*, 1998	13-7300 (rat brain)[4]	Und-1/100, ap		GAM
11. Rat Mouse	**Fix-para, Unfix**	**CaMKIIβ**	**Olf, VNO**	**Zymed; Wei *et al.*, 1998**	**13-9800 (rat brain)[4]**	**Und-1/100, ap**		**GAM**
12. Rat	Fix-para	CaMKII α	Olf	Zymed/Santa Cruz	13-7300/ SC-5391	1/10—1/100, ap		GAM/RAG
13. Rat	Fix-para	CaMKII β	Olf	Zymed/Santa Cruz	13-9800/ SC-1540	1/10—1/100, ap		GAM/RAG
14. Rat	**Fix-para, Fix-glu, Unfix**	**PDE1C2[3]**	**Olf, VNO**	**Dr. J. A. Beavo, University of Washington; Juilfs *et al.*, 1997**	**1 = 6584, GST[3], N[4]**	**1/10—1/10,000, Tw, serum**		**GAR, FAB, Pr G**
15. Rat	**Fix-para, Fix-glu, Unfix**	**PDE1C2**	**Olf, VNO**	**Dr. J. A. Beavo; Juilfs *et al.*, 1997**	**2 = 5061, GST, N[4]**	**1/10—1/10,000, Tw, serum**		**GAR, FAB**
16. Rat	**Fix-para, Fix-glu, Unfix**	**NKCC1/2[3]**	**Olf, VNO**	**Developmental Studies Hybridoma Bank, Univ. of Iowa, Iowa, City, IA; Lytle *et al.*, 1995**	**T4 (902-1212, C)[4]**	**Und-1/10, Tw, SDS[3], ap**		**GAM**
17. Rat	**Fix-para, Unfix**	**Supernatant non-IgG secreting cell**	**Olf**	**As above**	**T4 control; NS-1**	**1/3—1/10, Tw, SDS**		**GAM**
18. Rat	**Fix-para**	**NKCC1**	**Olf**	**Alpha Diagnostic San Antonio, TX**	**NKCC11-A, 22 amino acids, C**	**Und, ap**		**GAR**
19. Rat	Fix-para, Unfix	KCC2[3]	Olf	J. A. Payne, University of California, Davis; Wilson *et al.*, 1999	B22 pAB	Und-1/6, ap		GAR
20. Rat	**Fix-para, Unfix**	**$G^3_{olf\alpha}$, OMP[3]**	**Olf**	**OMP: Dr. F. L. Margolis, University of Maryland; $G_{olf\alpha}$: Menco *et al.*, 1994; Koo *et al.*, 2004[4,5]**	**Positive controls for GAR**	**1/5 ($G_{olf\alpha}$), ap; 1/100 (OMP), serum**		**GAR, RAG**

(*Continued on next page*).

Table 1. (*Continued*.)

A Species	B Fixation condition	C Antibody to	D Tissue	E Antibody source	F Antibody code	G Antibody dilutions and special conditions	H Peptide excess (w/w) for blocking	I Secondary probe[1]
21. Rat	**Unfix**	**1F4**	**Olf**	**Pixley *et al*., 1997[4,5]**	**Positive control for GAM**	**Und**		**GAM**
22. Rat	**Fix-para**	**–**	**Olf**	**–**	**Negative controls**	**–**		**GAR, RAG GAM**

1. All secondary probes were conjugated to 15-nm gold (Aurion, Electron Microscopy Sciences, Fort Washington, PA).
2. Bold = antibody worked; plain = antibody did not worked.
3. Para = freshly depolymerize paraformaldehyde; glu = freshly depolymerized paraformaldehyde supplemented with glutaraldehyde; Olf = olfactory; VNO = vomeronasal; GRK3 = G-protein receptor kinase type-3; CaMKII = Ca^{++}/calmodulin-dependent protein kinase II; PDE = phosphodiesterase; NKCC1 and NKCC2 = Na^+, K^+, Cl^--cotransporters; KCC2 = K^+, Cl^-- cotransporter; $G_{olf\alpha}$ = a G_α-type G-protein involved in vertebrate olfactory signaling; OMP = olfactory marker protein; C = C-terminal (plus antigenic peptide sequence, when available); N = N-terminal (plus antigenic peptide sequence, when available); Int = internal sequence (plus antigenic peptide sequence, when available); W = whole protein; GST = glutathione-S-transferase; Und = undiluted; SDS = sodium dodecyl sulfate; Tw = Tween 20; Bl Prot = Blue Carrier Protein® (Santa Cruz, sc-3725) used for conjugation of peptide in order to generate antibodies, here used in indicated excess in an attempt to suppress background; ap = affinity purified; GAR = goat-anti-rabbit; RAG = rabbit-anti-goat; GAM = goat-anti-mouse; FAB = goat-anti-rabbit F(ab') 2-fragment; Pr G = protein G.
4. These antibodies are the same as the ones used in earlier studies that formed the background for this fine-structural study. The Upstate antibody to GRK2/3 was the same as the one used in the earlier study (Dr. R. C. Lefkowitz, Personal communication; Dawson *et al*., 1993). The study by Wei *et al*. (1998) does not specify which of the two Zymed (α or β) antibodies to CaMKII was used, hence both were used and both are marked with a superscript. More extensive studies on NKCC1, including light microscopy, are in progress (Drs. N. K. Kleene and S. J. Kleene, Department of Cell Biology, Neurobiology, and Anatomy, University of Cincinnati, Cincinnati, OH; see also Resiert *et al*., 2005).
5. These references give the antibody source as well as additional results using the same antibodies. The OMP studies in Koo *et al*. (2004) were conducted in parallel with this study and in sections from the same tissues. No noticeable reduction of antigenic activity was seen in the OMP immunoreactivity in the stored tissues (see beginning Materials and methods).

Various procedures were used in order to try to reduce background. In several cases Tween 20 was included throughout the whole immunocytochemical procedure in all solutions apart from the final water wash (Tw, Column G in Table 1). The primary antibodies were also in some instances pre-incubated overnight at 4 °C with a vast excess of the protein that had been used by the commercial supplier for conjugation of the antigenic peptides, Blue Carrier Protein® (Bl Prot, Column G in Table 1). Inclusion of SDS for similar purposes (Table 1) led to removal of most of the sections in question from the grids. Therefore, SDS could not be used under our experimental conditions.

CONTROLS

When possible, specificity of antibody binding was verified by preabsorption with an excess of corresponding antigen in the immunocytochemical controls. Antibodies were incubated with antigenic peptide overnight at 4°C at the indicated excess (Column H in Table 1 and figure legends). Because of antibody efficacies and concentrations of antibodies and peptides supplied we were limited in the peptide excess that could be used. Tissue controls were receptor cell axons and surrounding tissue areas, supporting cell apices and microvilli, cell apices and microvilli of microvillous cells in the main olfactory epithelium, non-sensory cilia and microvilli of the nasal respiratory epithelium, and the sensory and non-sensory areas of the VNO. Previous studies of probes used for labeling of olfactory receptor cells (OMP; Koo *et al*., 2004; Menco, 1989) and receptor cell cilia ($G_{olf\alpha}$, Menco *et al*., 1992, 1994) and supporting cell microvilli (1F4, Pixley *et al*., 1997) served as additional tissue controls for the poly- (OMP, $G_{olf\alpha}$) and monoclonal antibodies (1F4; Lines 20 and 21 in Table 1). In the VNO, polyclonal antibodies to $G_{o\alpha}$ (Menco *et al*., 2001) were also used for this purpose. Moreover, the labeling pattern of each antibody was a positive control for all others and, in most cases, several antibodies were used to determine the consistency of labeling (Table 1, bold: positive results; plain: negative results, or antibodies that did not seem

Table 2. Olfactory signal-onset molecules and molecules of signal-termination and -regulation targeting these.

Signal-onset	***Odor receptors***	***$G_{olf\alpha}$***	***Type III AC***	***CNG-channels***	**Cl^--channels**
Signal-termination and -regulation	***GRK3, β-arrestin-2***		***PDE1C2, CaMKII***		***NKCC1***

Row 1: Sequentially activated onset molecules, from odorant receptor to current-generating channels. The fine structural locations of all but one (the chloride channel, hence, not in italics; Frings *et al*., 2000) of these signal-onset molecules had been the subject of earlier studies (reviewed in Menco & Morrison, 2003); all of these are concentrated in olfactory cilia.
Row 2: Molecules of signal termination and regulation putatively affecting those of signal-onset above (e.g., Nakamura, 2000, and text). These molecules, the fine structural locations of which are the subject of this study, also occur in olfactory cilia. In addition, they localize to dendritic knobs and apical regions, microvilli in particular, of neighboring supporting cells.

Table 3. A semi-quantitative summary of the fine-structural distribution of some molecules of olfactory signal-termination and -regulation in rat nasal epithelia.

Cells and subcellular compartments:	GRK3			β-Arrestin-2		CaMKII			
	Line 1[1] SC-9306	Line 2 SC-563	Line 3[2] G4665	Line 5 SC-13140	Line 6[2] A2 CT/7435-3	Line 7[2] SC-9035	Line 11 13-9800	PDE1C2 Lines 14 & 15[2,3] 6584/5061	NKCC1/2 Line 16[2,4] T4
Olfactory epithelial receptor cells:									
Cilia, distal parts	+[5]	+	++	+	++	+	+	++	+
Cilia, proximal parts	+	+	++	+	++	+	+	++	+
Dendritic knobs	+	±	++	+	+	+	+	++	+
Dendrites	−	±	+	±	±	±	±	+	+
Nuclei									−
Axons	−	±	±	±	±	±	±	−	+
Olfactory epithelial supporting cells:									
Microvilli	+	+	++	+	++	+	+	++	++
Apex	+	+	++	+	++	+	+	++	++
Deeper inside cells	±	±	+	±	+	−	−	−	++
Nuclei									−
Olfactory epithelial microvillous cells[6]:									
Microvilli	±	±	+	±	±	±	−	±	±
Apex	±	±	+	±	+	−	−	±	±
Deeper inside cells	±	±	±	−	±	±	−	−	±
Respiratory epithelial cells:									
Ciliated cells, cilia and microvilli	±	±	+	±	±	±	±	±	±
Ciliated cells, apex	±	±	±	−	±	−	±	±	±
Ciliated cells, deeper inside cells	±	±	±	−	±	−	−	±	±
Ciliated cells, nuclei									−
Goblet cells, microvilli and apex	+++								
Vomeronasal epithelial sensory cells:									
Microvilli			−		−	−		−	±
Apex			−		−	−		−	±
Deeper inside cells			−		−	−		−	±
Vomeronasal epithelial supporting cells:									
Microvilli			−		++	++		±	±
Apex			−		++	++		−	±
Deeper inside cells			−		−	−		−	±
Vomeronasal non-sensory epithelium:									
Ciliated cells, cilia and microvilli			−		−	−		−	±
Apex			−		−	−		−	±
Resin	−	−	−		−	−	−	−	−

1. The Line numbers refer to the different antibodies used as listed in Table 1. Only the catalogue or batch numbers are repeated here.
2. Evaluations in the VNO were based on these antibodies only.
3. The evaluations for both antibodies were pooled, as the same peptide was used to generate the antibodies, but in different rabbits (see Table 1)
4. Nuclei were included in the evaluation for the antibody to NKCC1/2 only, as here perinuclear cytoplasm was labeled. The nuclei were used for comparison with these cytoplasmic areas.
5. +++: very intense immunolabeling (only seen for goblet cells in respiratory epithelium for the antibody of Line 1 in Table 1). This labeling pattern was most likely non-specific, as preabsorption with peptide did not reduce the labeling intensity. ++: intense immunolabeling. +: moderate immunolabeling. ±: just noticeable immunolabeling. -: no apparent immunolabeling.
The evaluations for a particular antibody are based on averaging semi-quantitative scores for each condition and dilution for that particular antibody (see Materials and methods). Compare the labeling patterns depicted here for molecules of signal-termination and -regulation with those presented in Menco *et al.* (1994), Table 2, for molecules of olfactory signal-onset.
6. Microvillous cells included all cells with microvilli that differed from microvillous olfactory epithelial supporting cells (see Menco & Morrison, 2003).;

to work). Negative controls consisted of TBS/AcBSA and, in the case of monoclonal T4 antibodies, supernatant NS-1 of non-secreting IgG producing cells (Table 1) replacing the primary antibodies.

ELECTRON MICROSCOPY

Grids containing the immunolabeled sections were stained with 0.5% methanolic UAc, formvar- and carbon-coated on the tissue containing side, and examined at 100 kV in a JEOL 100 CX Temscan Transmission-Scanning or a JEOL1200 EX Transmission Electron Microscope (JEOL Ltd., Tokyo, Japan). Tissue blocks and sections (both before and after labeling) were stored in evacuated desiccators.

QUANTIFICATION

Olfactory receptor cell cilia and supporting cell microvilli mingle intimately, with their courses perpendicular to each other. In, e.g., Fig. 2, the distal parts of the receptor cell cilia had a course parallel to the short side of the micrograph (and the epithelial surface), whereas supporting cell microvilli had a course parallel to the long side of the micrograph. Moreover, same and nearby structures often had differing labeling intensities, as seen in, e.g., Fig. 17 for two neighboring dendritic endings that labeled differently for β-arrestin-2. Such differences were regularly encountered in the course of this work, for β-arrestin-2 as well as the other antibodies. Because of such overlap of labeled structures and variations in labeling intensity, and also because of the diversity of labeling conditions (Table 1, and the beginning of the Results), it was not feasible to numerically analyze the data, i.e., to assess densities of gold grains overlying olfactory cilia relative to surrounding areas. Instead, semi-quantitative evaluations were presented through the most prevalent patterns as noted in images of labeled structures (Table 3).

The semi-quantitative evaluations were carried out as follows. In each individual micrograph densities of gold particles overlaying structures of interest were scored with $-$, $\pm$, $+$, $++$, or $+++$ (see legend Table 3) for a particular antibody and labeling condition (conditions were, e.g., a certain dilution, inclusion of Tween 20, inclusion of Blue Carrier Protein® as described above). The total numbers of $+$ and $-$ signs were scored and divided by the number of photographs examined. Next, the scores for each condition of a particular antibody were averaged over the number of conditions. A minus-sign was assigned the value 0 and a $\pm-$ sign was assigned half a $+-$ sign.

Results

SOME GENERAL COMMENTS PERTINENT TO ALL LABELING PROCEDURES

Table 2 serves as a guide as to where in the cascade of olfactory signaling to place the various molecules investigated here (see also the references to reviews listed in the Introduction). Variations in methods included: 1. *Tissue preparation*. All micrographs included are based on tissues that were fixed with freshly depolymerized paraformaldehyde before cryoprotection and freeze-substitution. Unfixed tissues gave no distinct labeling pattern for any of the antibodies used (Table 1). This contrasts sharply with some of our studies with other antibodies, in which unfixed tissues labeled as well or better than fixed ones, sometimes even exclusively (e.g., Menco *et al.*, 1992, 1994, 1998; Menco, 1995; Pixley *et al.*, 1997). Also, within this study, although inclusion of 0.1% glutaraldehyde sometimes did give a labeling pattern, immunocytochemical results with freshly depolymerized paraformaldehyde fixation alone were superior and all results presented here are based on material obtained using the latter fixative only. 2.

Fig. 1. Section through the surface of rat olfactory epithelial tissue fixed with freshly depolymerized paraformaldehyde and cryoprotected before freeze-substitution. The section was incubated with antibodies to GRK3 at a dilution of 1:10 and the antibody incubation medium included Tween 20 (Tw) throughout the whole procedure. The secondary probe was RAG-gold (15 nm) (GRK3-RAG; Line 1 in Table 1). A dendritic ending (d) of an olfactory receptor cell shows less labeling than the thick proximal (pc) and the long and thinner distal parts (dc) of the receptor cell cilia. Apices (s) and microvilli (mv) of neighboring supporting cells also labeled (see also Figs. 2, 3, 6 and 8). Scale bar = 1 μm.

Fig. 2. Section through the surface of rat olfactory epithelial tissue prepared as described in the legend of Fig. 1, but the section was exposed to an other, different, antibody to GRK3, undiluted and also with Tween 20 (und Tw) included throughout the whole procedure. The secondary probe was GAR-gold (15 nm) (GRK3-GAR; Line 2 in Table 1). Proximal (pc) and distal parts (dc) of the cilia of olfactory receptor cells and supporting cell microvilli (mv) labeled, but the dendritic ending (d) and supporting cell apices (s) did not (compare with Fig. 3). Scale bar = 1 μm.

Fig. 3. A different section through the surface of rat olfactory epithelial tissue, treated as the one shown in Fig. 2. Distal parts of olfactory cilia (dc, arrowheads) and supporting cell microvilli (mv, asterisks) are seen labeled; microvilli (miv) and apex (mi) of a neighboring cell that resembles a hair-cell like microvillous cell (Menco & Jackson, 1997) lacked labeling. The inset depicts a nearby section (area of circle in main figure), to show consistency of labeling (compare with Fig. 2). d = Dendritic ending, pc=proximal parts of olfactory cilia, s=supporting cell apex. Scale bar = 1 μm.

Fig. 4. Axons below the surface area of Figs. 2 and 3. These axons were devoid of labeling. Compare especially with the receptor cell cilia seen labeled in Figs. 2 and 3, and with the axonal labeling pattern using a different antibody to GRK3 as seen in Fig. 9. Scale bar = 1 μm.

Fig. 5. Using the same antibody as employed in Figs. 2–4 and under similar experimental conditions, respiratory cilia show only a few gold grains (e.g., arrowhead; compare especially with the receptor cell cilia seen labeled in Figs. 2 and 3). Scale bar = 1 μm.

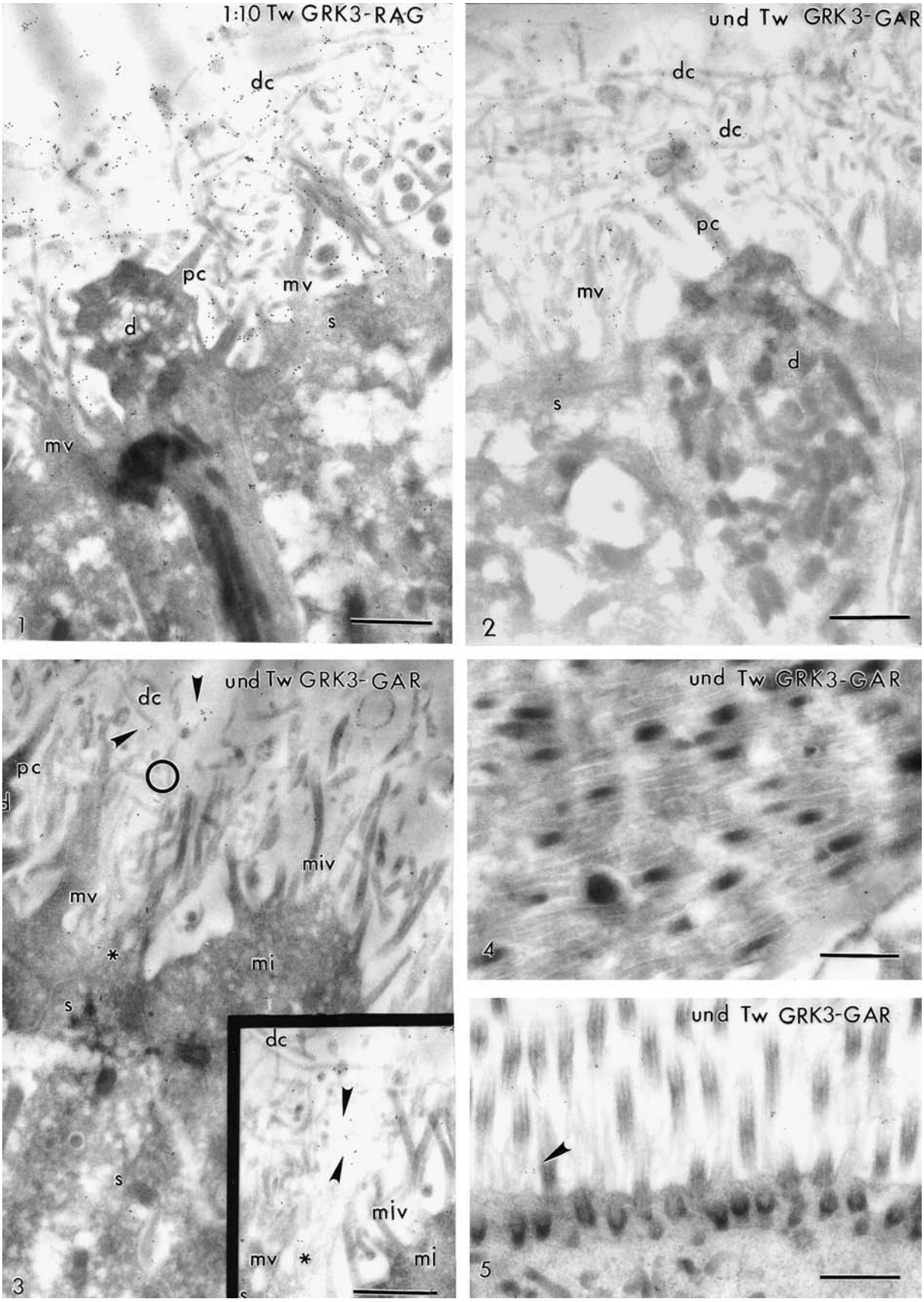
1:10 Tw GRK3-RAG
dc
pc
mv
d
s
mv
1
und Tw GRK3-GAR
dc
dc
pc
mv
d
s
2
und Tw GRK3-GAR
dc
pc
miv
mv
*
mi
s
s
dc
miv
mv
*
mi
3
und Tw GRK3-GAR
4
und Tw GRK3-GAR
5

Antibody selection. Some of the same antibodies that were employed in earlier, light-microscopic investigations provided the background for this ultrastructural one. Though indicative, the labeling patterns obtained were often not sufficiently distinct to allow an immediate verdict. To supply firmer evidence for these patterns we used additional antibodies to those employed in the earlier investigations for most antigens (Introduction and Table 1). Other variations included 3. *dilutions* and 4. *blocking procedures* (Table 1 and figure legends). Preabsorption with a protein used for conjugation of antigens in the generation of some of the antibodies, Blue Carrier Protein, where applied (Lines 1, 2, and 5 in Table 1), did not markedly alter the pattern of labeling for any of the antibodies. This suggests that background was not caused by a presence of antibodies generated to Blue Carrier Protein (an unlikely event as the antibodies in question were affinity purified). 5. *Detergent*. Inclusion of Tween 20 throughout the whole immunolabeling procedure markedly reduced the overall intensity of labeling. However, its inclusion did help to clarify some of the results, notably those for GRK3 and NKCC1/2 (Lines 1–3 and 16–18 in Table 1).

GRK3

Three of the four antibodies that were used to demonstrate the fine-structural localization of GRK3 yielded results (Lines 1, 2 and 4 in Table 1; Figs. 1–11). With all three antibodies, labeling was restricted to the epithelial surface, where olfactory cilia and supporting cell microvilli immunoreacted well with the antibodies of Lines 1 and 2 in Table 1 (Figs. 1–3; Table 3). In some images cilia seemed to display more labeling (e.g., Fig. 3), whereas in others, using the same antibody, supporting cell microvilli had more gold particles (Fig. 5). The inset of Fig. 3 shows that the labeling pattern is consistent between neighboring sections. For both of these antibodies, labeling was more intense in the rat than in the mouse (mouse not shown). The antibody of Line 1 (Table 1) tended to give more background, hence most of the images presented are those obtained with the antibody of Line 2. The same antibody used in a light-microscopic study (Dawson *et al*., 1993) to demonstrate the location of GRK3 in olfactory epithelia (Line 4 in Table 1) was an antibody to a region common to GRK2 and GRK3. This antibody labeled dendritic endings and proximal and distal parts of olfactory cilia equally well (Fig. 8; Table 3). Another monoclonal antibody against the same epitope, but from a different commercial source, did not work (Line 3 in Table 1). Under identical experimental conditions structures below the immediate cell surfaces barely immunoreacted (Figs. 1–3, 6–8), and this included cell bodies (not shown, but see Figs. 1-3 for supranuclear regions) as well as the area around the basal lamina and receptor cell axons and surrounds (Figs. 4 and 9; Table 3). Immunoreactivity of the microvilli of microvillous cells,

Fig. 6. Section through the surface of rat olfactory epithelial tissue prepared as described in the legend of Fig. 1. The section was incubated with anti-GRK3 at a dilution of 1:5 with Tween 20 (Tw) present throughout the whole procedure. The secondary probe was GAR-gold (15 nm) (GRK3-GAR; Line 2 in Table 1). Supporting cell microvilli (mv; e.g., near asterisk) and proximal (pc) and distal parts of receptor cell cilia (dc, arrows) are seen labeled. d = Dendritic ending, s = supporting cell apex, s = supporting cell apex. Scale bar = 1 μm.

Fig. 7. Section through the surface of rat olfactory epithelial tissue as described in the legend of Fig. 6, but a peptide control where antibody at a dilution of 1:5 was preabsorbed overnight with a five-fold excess (by weight) of antigenic peptide (pept). Though slightly reduced, labeling could not be completely eliminated and displayed the same pattern as that seen in Fig. 6. d = Dendritic ending, pc = proximal parts of olfactory cilia, dc = distal parts of olfactory cilia, s = supporting cell apex, mv = supporting cell microvilli. Scale bar = 1 μm.

Fig. 8. Section through the surface of rat olfactory epithelial tissue prepared as described in the legend of Fig. 1, but incubated with a different antibody (monoclonal), now to GRK2/3 at a dilution of 1:250, with GAM as the gold (15 nm)- conjugated secondary probe (GRK2/3-GAM; Line 4 in Table 1). The primary antibody was the same as that used in an earlier, light-microscopic, study on the location of GRK3 in olfactory epithelia (Dawson *et al*., 1993). Dendritic endings (d) and proximal (pc) and distal parts of cilia (dc, near asterisk) of receptor cells as well as microvilli of supporting cells (mv) are seen labeled. Microvilli (miv) of a nearby microvillous cell (mi) Type 2 (Menco & Morrison, 2003) did not label. s = Supporting cell apex, mi = apex microvillous cell. Scale bar = 1 μm.

Fig. 9. Section through olfactory receptor cell axons incubated with an antibody to GRK2/3 as described in the legend of Fig. 8. The axons did not label (see also Fig. 4). Scale bar = 1 μm.

Fig. 10. Section through rat VNO sensory epithelium prepared in the same way as the olfactory tissues (see legend Fig. 1) incubated with an antibody to GRK2/3 as described in the legend of Fig. 8. Labeling was absent in apices (d = dendrite; s = supporting cell) and microvilli of both receptor (mr) and supporting cells (ms; the fatter microvilli that are oriented perpendicular to the epithelial surface). The arrowheads outline the epithelial surface. Scale bar = 1 μm.

Fig. 11. Section through rat VNO non-sensory epithelium prepared in the same way as the olfactory tissues (see legend Fig. 1) incubated with an antibody to GRK2/3 as described in the legend of Fig. 8. Cilia (c) and microvilli (m) did not immunoreact. Scale bar = 1 μm.

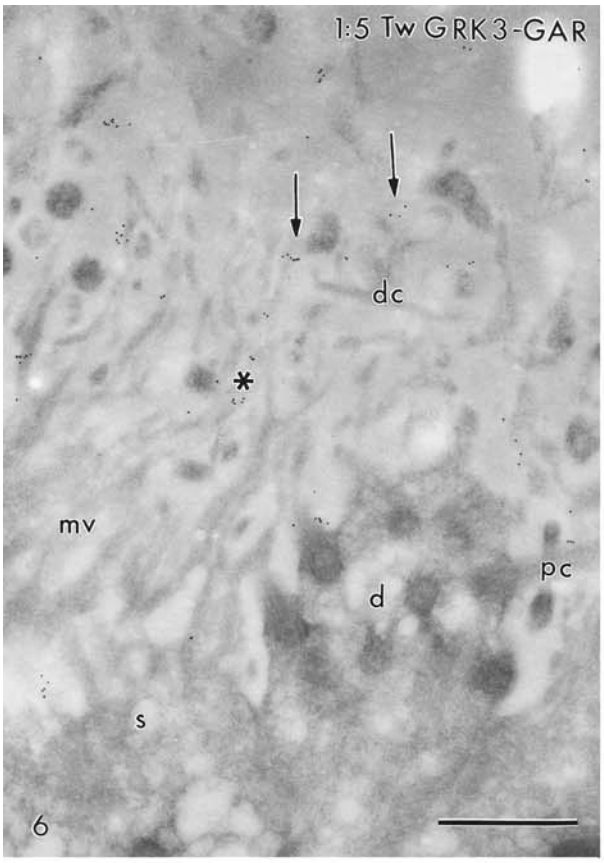
1:5 Tw GRK3-GAR
dc
*
mv
pc
d
s
6

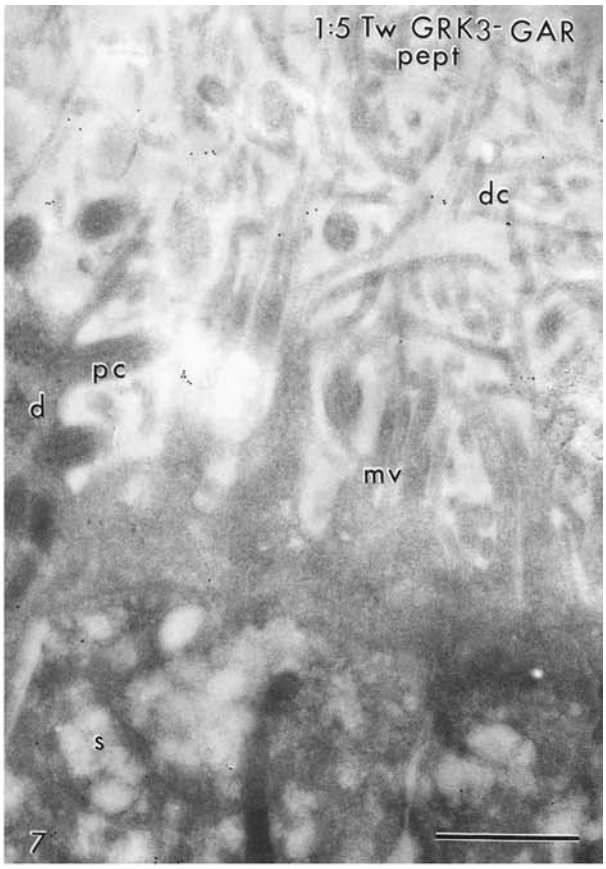
1:5 Tw GRK3- GAR
pept
dc
pc
d
mv
s
7

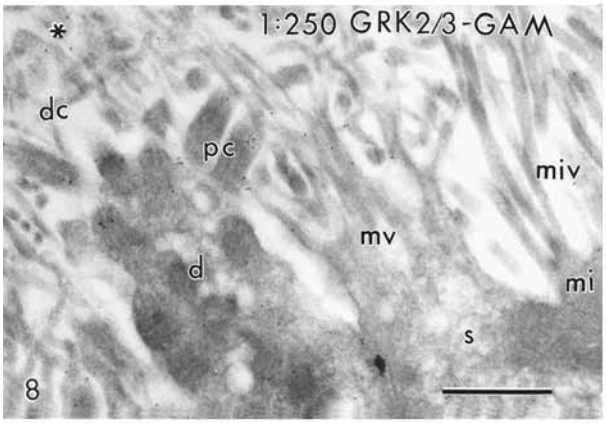
*
1:250 GRK2/3-GAM
dc
pc
miv
mv
d
mi
s
8

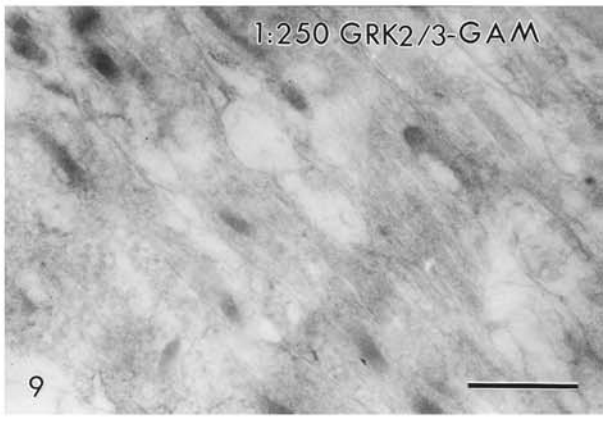
1:250 GRK2/3-GAM
9

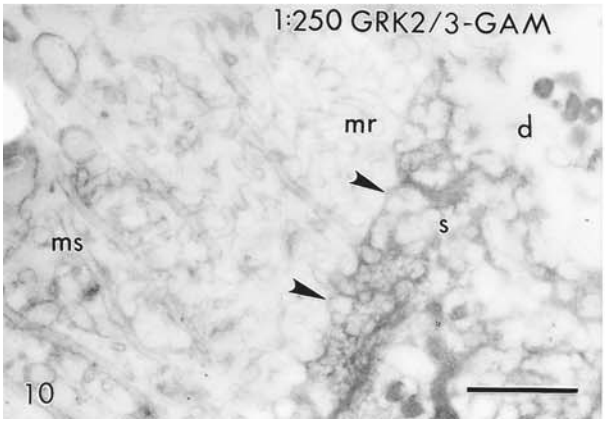
1:250 GRK2/3-GAM
mr
d
s
ms
10

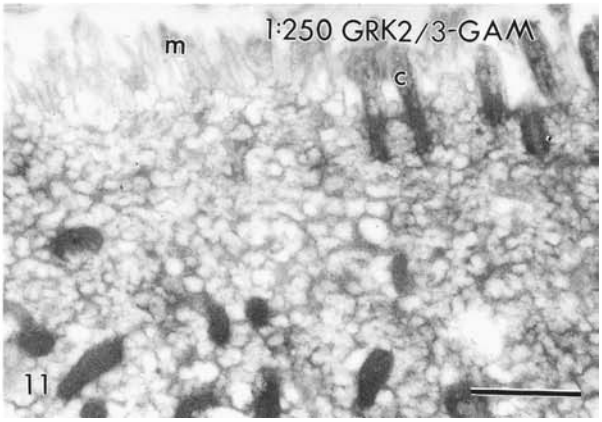
m
1:250 GRK2/3-GAM
c
11

which are not typical supporting cells (Figs. 3 and 8; review: Menco & Morrison, 2003), and of respiratory cilia was sparse (Fig. 5) for all three antibodies that worked well in apical regions of olfactory epithelial receptor and supporting cells (Table 3).

Preabsorption with an excess of peptide, used to generate the GRK3 antibodies, resulted in a diminished but not abolished labeling (Figs. 6 and 7 for the antibody of Line 2 in Table 1). Because of antibody efficacy we could not use an excess of a peptide concentration above 5× peptide to 1× antibody (weight/weight), which may be a reason why immunoreactivity could not be totally blocked. Reduction in labeling intensity was also noted for the antibody of Line 1 in Table 1 when the antibody was presabsorbed with a twenty-fold excess of antigen (dilution of 1:20, Tween 20 throughout). This antibody heavily labeled a respiratory epithelial goblet cell secretory substance. However, preabsorption did not give reduced immunoreactivity of this substance, suggesting that labeling of these goblet cells is non-specific (image not shown, but see Table 3).

The antibody of Line 4 (Table 1) was also applied to the rat's VNO, where structures in the sensory (Fig. 10) and non-sensory (Fig. 11) epithelial surfaces, incubated under the same conditions as Figs. 8 and 9, remained unlabeled (Table 3), as was true for VNO receptor cell axons (not shown, but see Fig. 28). The data are summarized in Table 3.

β-ARRESTIN-2

The pattern of labeling with two antibodies to β-arrestin-2 (Lines 5 and 6 in Table 1; Figs. 12–19) was quite similar to that seen for antibodies to GRK3 (Figs. 1–11; Table 3). Labeling was restricted to the olfactory epithelial surface where receptor-cell dendritic endings and their cilia, as well as apices and microvilli of supporting cells, were seen labeled (Figs. 12, 15, and 17). Labeling was virtually absent below the surfaces; this included cell bodies, as well as axons of receptor cells (Figs. 13 and 18). Immunoreactivity was negligible in apices and microvilli of several types of microvillous cells (Menco & Morrison, 2003). Fig. 17 shows this for the antibody of Line 6 in Table 1. The same is true for respiratory cilia (Figs. 14 and 19; Table 3). The labeling pattern in mouse (not shown) was essentially the same as in rat. Preabsorption of the antibody with an excess of antigenic peptide (Line 5 in Table 1) reduced, but not abolished, the intensity of labeling (Figs. 15 and 16). As mentioned above for GRK3, limited antibody efficacy may be the reason that immunoreactivity could not be totally abolished (5× peptide to 1× antibody, weight/weight).

One of the two antibodies was also applied to VNO epithelial tissue (Line 6 in Table 1), where supporting cell apices and microvilli were seen labeled while receptor-cell structures, including their microvilli (Fig. 20) and axons (not shown, but see Fig. 28), did not show immunoreactivity (Table 3). Labeling was absent from cilia and microvilli of cells in the non-sensory region of the VNO as well (Fig. 21; Table 3).

CAMKII

The pattern of labeling with two antibodies to CaMKII in the olfactory epithelial surface was rather similar to that seen for GRK3 (Figs. 1–11) and β -arrestin-2 (Figs. 12–21; Table 3). One antibody was polyclonal, generated to an antigen common to α and β subunits of CaMKII; the other one was monoclonal and specific to the β subunit alone (Lines 7 and 11 in Table 1; Figs. 22–32). Three other antibodies to CaMKII α and β subunits did not give results (Lines 8–10 in Table 1) even when antibodies from two different sources to either CaMKII α or β subunits were administered together (Lines 12 and 13, respectively, in Table 1). Curiously the antigenicity to the Zymed antibody to CaMKII β (Line 11, Table 1) disappeared when administered

Fig. 12. Section through the surface of rat olfactory epithelial tissue fixed with freshly depolymerized paraformaldehyde and cryoprotected before freeze-substitution, incubated with a monoclonal antibody to β-arrestin-2, undiluted, with GAM as the gold (15 nm)-conjugated secondary probe (und arr-GAM; Line 5 in Table 1). Labeling was mostly restricted to the surface where dendritic endings (d), proximal (pc) and distal parts of olfactory cilia (dc), and supporting cell apices (s) and microvilli (mv) immunoreacted (compare with Figs. 15 and 17). Scale bar = 1 μm.

Fig. 13. Section through rat olfactory receptor cell axons incubated with a monoclonal antibody to β-arrestin-2 as described in the legend of Fig. 12. There is virtually no labeling (see also Fig. 18). Scale bar = 1 μm.

Fig. 14. Section through rat respiratory epithelial surface incubated with a monoclonal antibody to β-arrestin-2 as described in the legend of Fig. 12. Cilia immunoreacted with the antibody (see also Fig. 19). Scale bar = 1 μm.

Fig. 15. Section through the surface of rat olfactory epithelial tissue prepared as described in the legend of Fig. 12, but incubated with a monoclonal antibody to β-arrestin-2 at a dilution of 1:5. Receptor (d) and supporting cell apical structures (s), including proximal (pc) and distal (dc) parts of the olfactory cilia and supporting cell microvilli (mv), are seen labeled (compare with Fig. 16). s = Supporting cell apex. Scale bar = 1 μm.

Fig. 16. When exposed to antibody preabsorbed overnight with a five-fold excess of antigenic peptide (by weight; pept), the intensity of labeling was reduced, though not abolished (compare with Fig. 15). d = Dendritic ending, pc = proximal parts of olfactory cilia, dc = distal parts of olfactory cilia, s = supporting cell apex, mv = supporting cell microvilli. Scale bar = 1 μm.

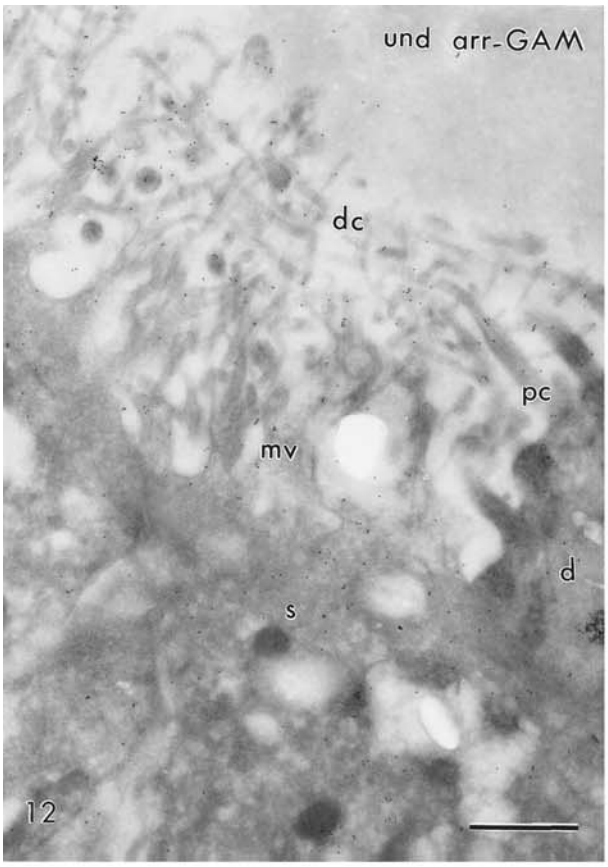
und arr-GAM
dc
pc
mv
d
s
12

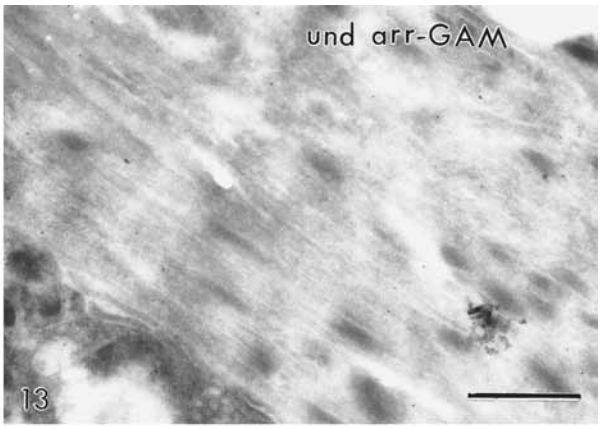
und arr-GAM
13

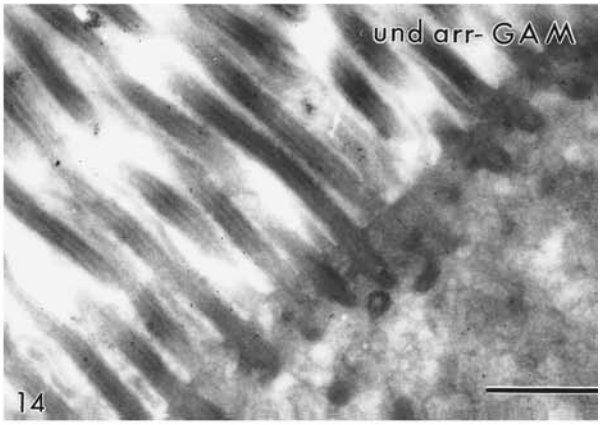
und arr- GAM
14

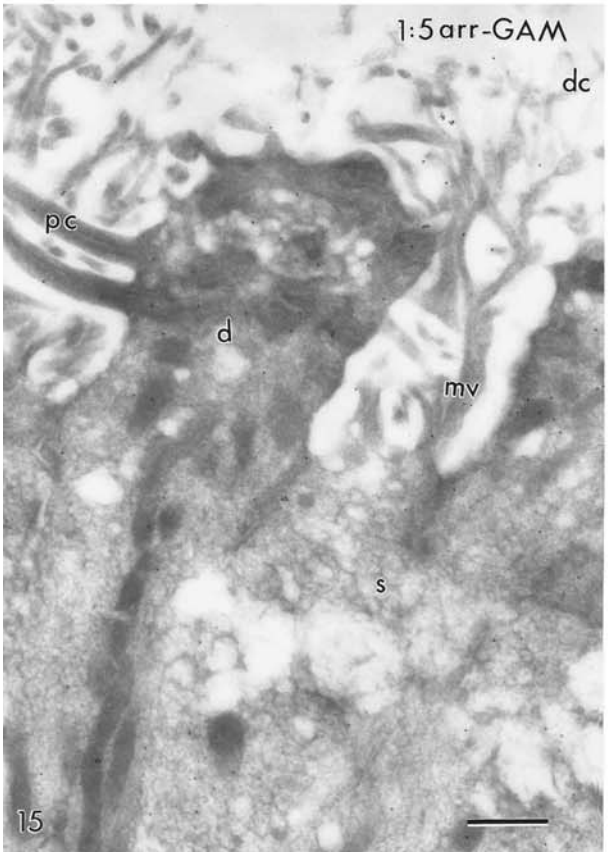
1:5 arr-GAM
dc
pc
d
mv
s
15

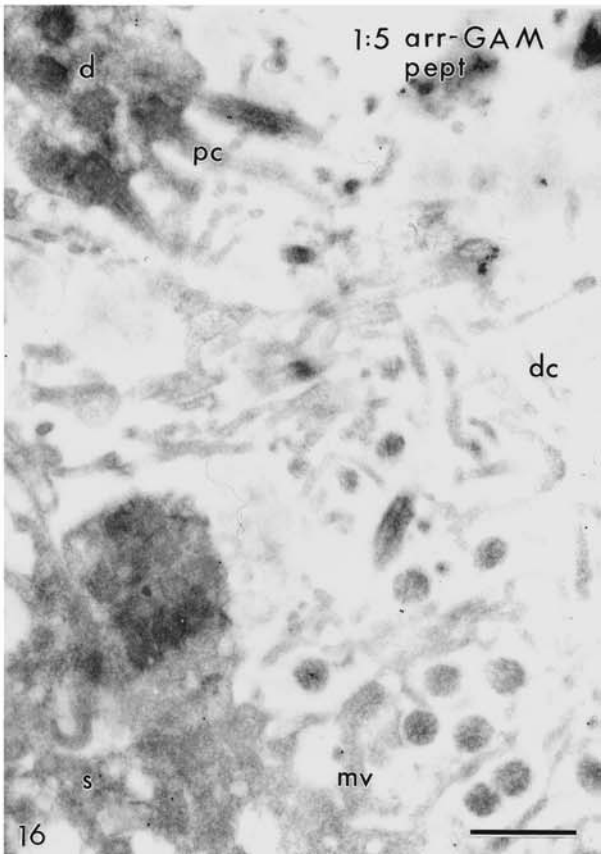
1:5 arr-GAM
pept
d
pc
dc
s
mv
16

together with the Santa Cruz antibody to CaMKII β of Line 9 (Table 1). In the epithelial surface, supporting cell apices and microvilli as well as dendritic endings and proximal and distal segments of olfactory cilia all labeled (Figs. 22–24, and 30; Table 3). As before for GRK3 and β -arrestin-2, the labeling intensity tapered off just below the epithelial surface. The labeling intensity was much lower in the axons of the receptor cells and their surrounds (Figs. 23 and 31) than in the epithelial surface (Figs. 22–24, and 30). Under the same conditions used for demonstrating CaMKII immunoreactivity in olfactory epithelial surfaces (Figs. 22 and 30), respiratory cilia immunoreacted only slightly (Figs. 26 and 32). The same was true for microvilli of microvillous cells, which labeled negligibly compared to surrounding supporting cells (Fig. 23; Table 3), similar to the results for GRK3 (Figs. 3 and 8) and β- arrestin-2 (Fig. 17).

The pattern of labeling in the sensory (Figs. 27 and 28) and non-sensory regions of the VNO (Fig. 29) was similar to that seen for β-arrestin-2 (Figs. 20 and 21). In particular, microvilli and apices of VNO supporting cells labeled prominently, even more so than structures in olfactory epithelia (compare Fig. 27, VNO, with Fig. 22, olfactory area, where the same conditions were used; Line 8 in Table 1, see also Table 3). Neither the receptor cell structures (Figs. 27 and 28) nor the structures in the surface of the non-sensory VNO epithelium immunoreacted (Fig. 29).

PDE1C2

Two polyclonal antibodies against the same epitope, but generated in different rabbits, were used to localize the Ca^{2+}/calmodulin-dependent phosphodiesterase, PDE1C2 (Figs. 33–38; Lines 14 and 15 in Table 1). Though both of them gave the same pattern of labeling they did so with differing efficacies, the one of Line 15 having the higher effectiveness. The pattern of labeling was essentially the same as that seen for GRK3, β-arrestin-2, and CaMKII (Table 3). Both immunoreacted exclusively with epithelial surfaces, where distal and proximal parts of olfactory receptor cell cilia, dendritic endings, and supporting cell microvilli and apices were seen labeled (Figs. 33–35 and 38; Table 3). Labeling was not present below the immediate surfaces of the cells, as shown for axons that did not label (Fig. 36) under the same experimental conditions as those used for the epithelial surface area of Fig. 35. Respiratory cilia (Fig. 37) and microvilli of microvillous cells labeled sparsely (Fig. 38).

Both antibodies were also applied to the VNO where no labeling was found, even in the absence of Tween 20 (not shown but see Table 3).

A technical note: results were similar using GAR or GAR-FAB as a secondary probe (compare Figs. 33 and 35).

Cl^--COTRANSPORTER

Three antibodies were used to localize Cl^--cotransporters, one common to NKCC1 and NKCC2 (T4, Line 16 in Table 1), one to NKCC1 (Line 18 in Table 1), and one to KCC2 (Line 19 in Table 1). Results with the latter were negative. As NKCC2 is only found in kidney (Sands, 2004) and there is no mRNA for NKCC2 in the olfactory epithelium (Kaneko

Fig. 17. Section through the surface of rat olfactory epithelial tissue prepared as described in the legend of Fig. 12, but with a different antibody to β-arrestin-2 that was applied at a dilution of 1:250, with GAR as the gold (15 nm)-conjugated secondary probe (arr-GAR; Line 6 in Table 1). The primary antibody was the same as that used in an earlier, light-microscopic, study on the location of β-arrestin-2 in olfactory epithelia (Dawson *et al.*, 1993). Immunoreactivity was mostly restricted to the epithelial surface where dendritic endings (d), proximal (pc) and distal segments of olfactory cilia (d), and supporting cell apices (s) and microvilli (mv) labeled. Note that labeling in the dendritic ending marked with a small asterisk is more intense than in the one to the right of it, marked with a larger asterisk. Apex (mi) and microvilli (miv) of a nearby microvillous cell Type 2 (Menco & Morrison, 2003) show only minimal labeling. Scale bar = 1 μm.

Fig. 18. Section through rat olfactory receptor cell axons exposed to the same antibody as used for Fig. 17. Labeling was virtually absent, even at an antibody concentration 2.5 times (1:100 instead of 1:250) as high as that used in Fig. 17. Scale bar = 1 μ m.

Fig. 19. Section through rat respiratory epithelial surface exposed to the same antibody as used for the section seen in Fig. 17. Respiratory cilia labeled slightly with this antibody to β-arrestin-2, and much less so than olfactory epithelial surface structures, even at an antibody concentration 2.5 times (1:100 instead of 1:250) as high as that used in Fig. 17. The resin did not label, and with the other antibody to β-arrestin 2 (Fig. 14) respiratory cilia labeled quite well, suggesting that the immunoreactivity of respiratory cilia for β-arrestin 2 is genuine and not background. Scale bar = 1 μm.

Fig. 20. Section through rat VNO sensory epithelium prepared in the same way as the olfactory tissues (see legend Fig. 1), incubated with an antibody to β-arrestin-2 at a dilution of 1:250, with GAR as the gold (15 nm)-conjugated secondary probe (arr-GAR; Line 6 in Table 1). Apices (s) and microvilli (ms) of supporting cells labeled abundantly, but labeling was absent from receptor cell dendrites (d) and microvilli (mr). The arrowheads roughly outline the epithelial surface (compare with Fig. 27). Scale bar = 1 μm.

Fig. 21. Section through rat VNO non-sensory epithelium prepared in the same way as the olfactory tissues (see legend Fig. 1). There is no noticeable labeling (compare with Fig. 29). c = Cilia, m = microvilli. Scale bar = 1 μm.

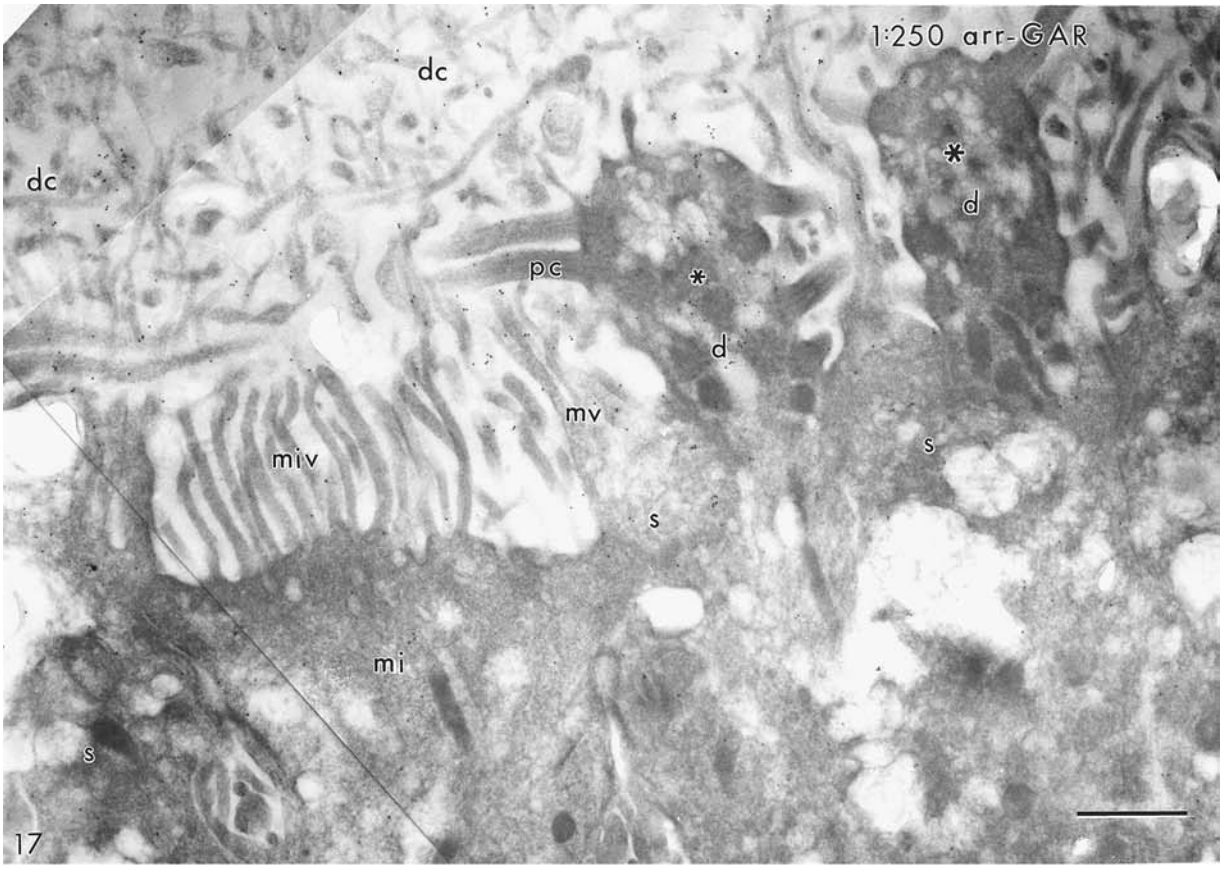
1:250 arr-GAR
dc
dc
pc
*
*
d
d
mv
miv
s
s
mi
s
17

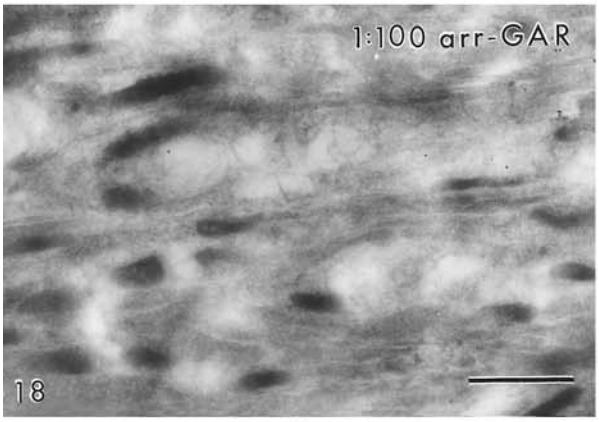
1:100 arr-GAR
18

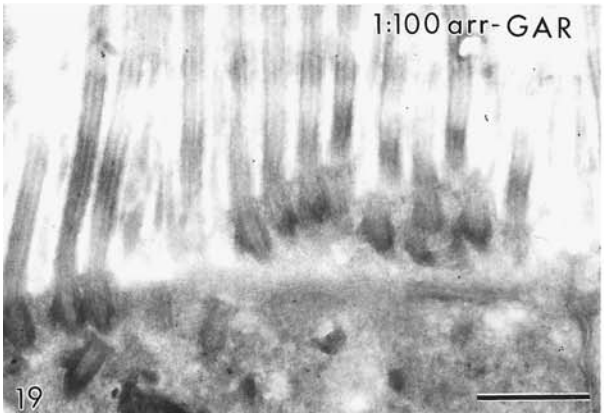
1:100 arr-GAR
19

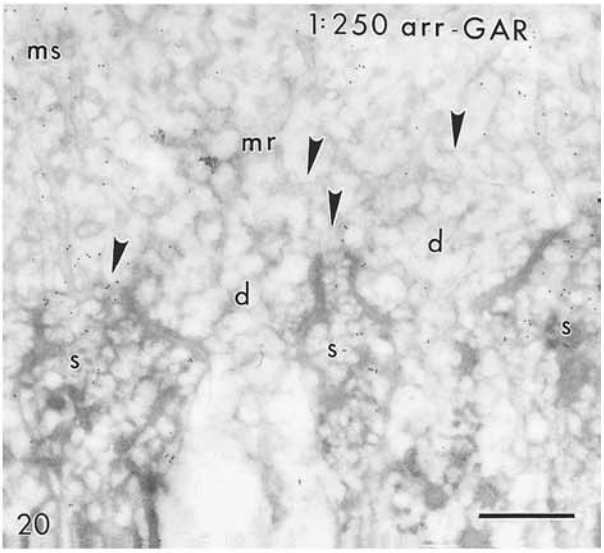
1:250 arr-GAR
ms
mr
d
d
s
s
s
20

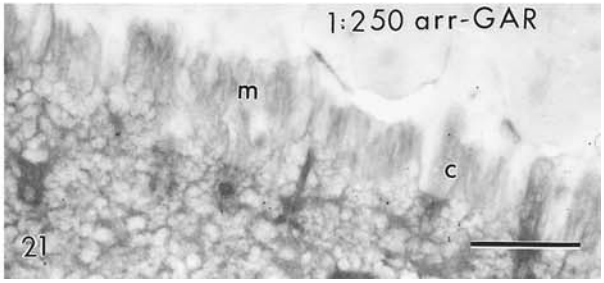
1:250 arr-GAR
m
c
21

et al., 2004) consideration is limited to NKCC1. The micrographs and data presented in Table 3 are based on the monoclonal antibody to NKCC1/2 (Figs. 39–47). The few data obtained with the polyclonal antibody to NKCC1 were essentially similar to those obtained with the monoclonal antibody to NKCC1/2. In the epithelial surfaces the results were comparable to those obtained with the antibodies used to demonstrate sites of olfactory signal-termination, in that both receptor and supporting cell structures showed immunoreactivity (Fig. 39; Table 3). With this antibody, however, immunoreactivity extended throughout the cytoplasms of both olfactory epithelial supporting and receptor cells (Figs. 40 and 41), including the axons of the latter (Fig. 42). Cilia of respiratory cells labeled as well (Fig. 43), and here too immunoreactivity extended into the cell's cytoplasm (Fig. 44). In all cases, cell nuclei were devoid of labeling (Figs. 40, 41, and 44; Table 3). The supranuclear area of supporting cells labeled especially well (Fig. 40). As was true for all other antibodies used, microvilli of microvillous cells immunoreacted sparsely (Figs. 45 and, especially, 47). The same was true for apical structures of VNO sensory and non-sensory epithelia (not shown, but see Table 3). When the sections were incubated with supernatant NS1 that did not contain the NKCC1/2 antibodies present in T4, labeling was absent (Fig. 46).

ADDITIONAL CONTROLS

Several controls additional to the ones included above were conducted. As positive controls, we used antibodies previously studied in olfactory epithelial tissues, i.e., those to $G_{olf\alpha}$ (Menco *et al*., 1992, 1994), OMP (Koo *et al*., 2004), and 1F4 (Pixley *et al*., 1997). Labeling patterns for these proteins were consistent with those described in the above-mentioned earlier publications. Also, the published results on the fine-structural localization of proteins of olfactory signal-onset—notably those to odor receptors (Menco *et al*., 1997), the G-protein subunits $G_{olf\alpha}$ and $G_{s\alpha}$, ACIII (Menco *et al*., 1992, 1994), and a cyclic-nucleotide-gated channel subunit (CNGA2, formerly called OCNC1; Kaupp & Seifert, 2002; Matsuzaki *et al*., 1999) in the main olfactory organ and to $G_{i\alpha 2}$, $G_{o\alpha}$ and TRP2 in the VNO (Menco *et al*., 2001)—served as positive controls (reviewed in Menco, 1997, 2003). The overall pattern of labeling with these antibodies to proteins of signal-onset displayed a major difference from the results reported here for the molecules of signal- termination and -regulation in that all of the antibodies to signal-onset molecules immunoreacted exclusively with receptor cell structures, distal parts of olfactory cilia (main olfactory organ) and receptor cell microvilli VNO in particular, whereas none reacted with supporting cell structures. And, ultrastructurally, with some exceptions, e.g., odor receptors (Menco *et al*., 1997), antibodies to most signal-onset proteins (reviews, Menco, 1995, 1997, 2001), worked well in fixed and unfixed tissues, while all of those used here required chemical fixation of the tissues to be labeled.

Negative controls, needed to assess the stability of the immunogold label, were regularly conducted. In the absence of primary antibodies, the secondary ones did not label for any of the secondary gold-conjugated probes, shown here (for GAR, Fig. 48, but the situation for RAG and GAM was the same), suggesting that these probes were adequate.

Discussion

This study showed that the fields of labeling for antibodies to molecules of signal termination (GRK3,

Fig. 22. Section through the surface of rat olfactory epithelial tissue fixed with freshly depolymerized paraformaldehyde and cryoprotected before freeze-substitution, incubated with a polyclonal antibody to CaMKII α/β, at a dilution of 1:10, and with GAR as the gold (15 nm)-conjugated secondary probe (CAMK-GAR; Line 7 in Table 1). Immunoreactivity included dendritic endings (d) and proximal (pc) and distal parts of olfactory cilia (dc) as well as supporting cell apices (s) and microvilli (mv). Deeper in the epithelium (asterisk), labeling was minimal (compare with Figs. 23 and 24). Scale bar = 1 μm.

Fig. 23. Section through the surface of rat olfactory epithelial tissue prepared as described in the legend of Fig. 22, and immunoreacted with the same antibody to CaMKII α/β, but at a dilution of 1:2. Compare this labeling pattern with that seen in Fig. 22, where the antibody was 5 times the dilution used here. Apices (s) and microvilli (mv) of supporting cells, receptor cell dendritic endings (d), and proximal (pc) and distal parts of olfactory cilia (dc) labeled well, in contrast to the lack of labeling of the microvilli (miv) of a microvillous cell Type II (mi). Scale bar = 1 μm.

Fig. 24. Section through the surface of rat olfactory epithelial tissue prepared as described in the legend of Fig. 22, incubated with the same polyclonal antibody as used for the image of Fig. 22, but undiluted and with Tween 20 present throughout the whole procedure (und Tw CAMK-GAR). The labeling pattern resembles that seen in Fig. 22. d = Dendritic ending, pc = proximal parts of olfactory cilia, dc=distal parts of olfactory cilia, s = supporting cell apex, mv = supporting cell microvilli. Scale bar = 1 μm.

Fig. 25. Section through rat olfactory receptor cell axons exposed to the same CaMKII α/β antibody and conditions as used for the section of Fig. 24. Labeling was virtually absent (compare with Figs. 28 and 31). Scale bar = 1 μm.

Fig. 26. Section through rat respiratory epithelial surface exposed to the same antibody and incubation conditions as used for the section seen in Fig. 24. Labeling was virtually absent. Scale bar = 1 μm.

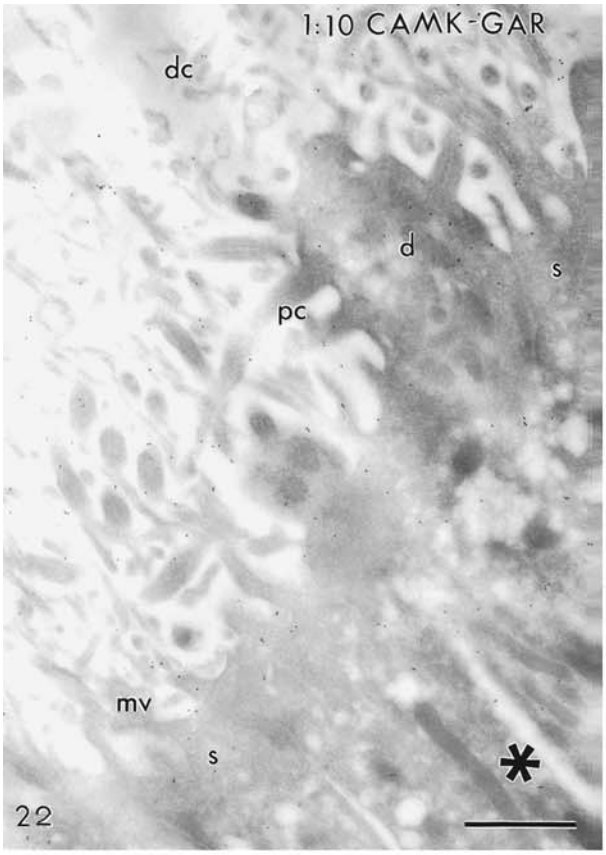
1:10 CAMK-GAR
dc
d
s
pc
mv
s
*
22

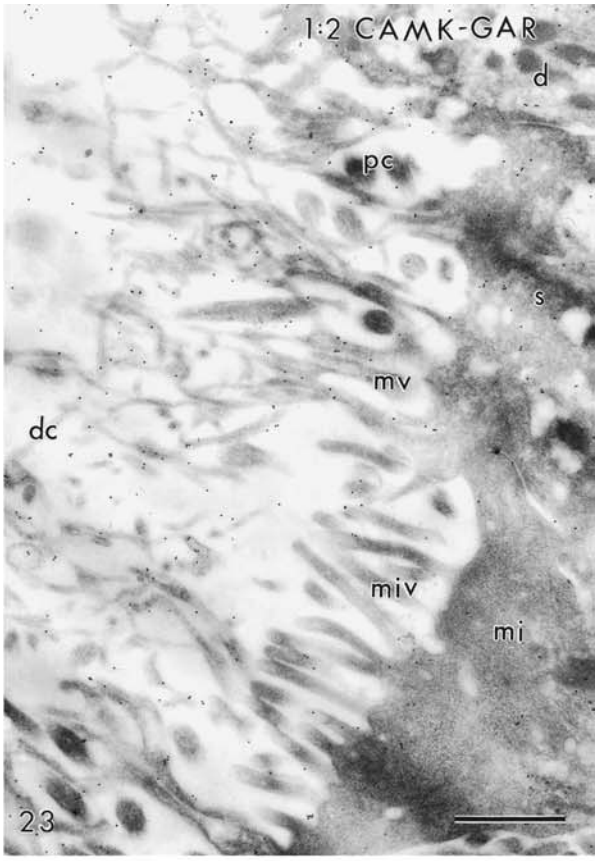
1:2 CAMK-GAR
d
pc
s
mv
dc
miv
mi
23

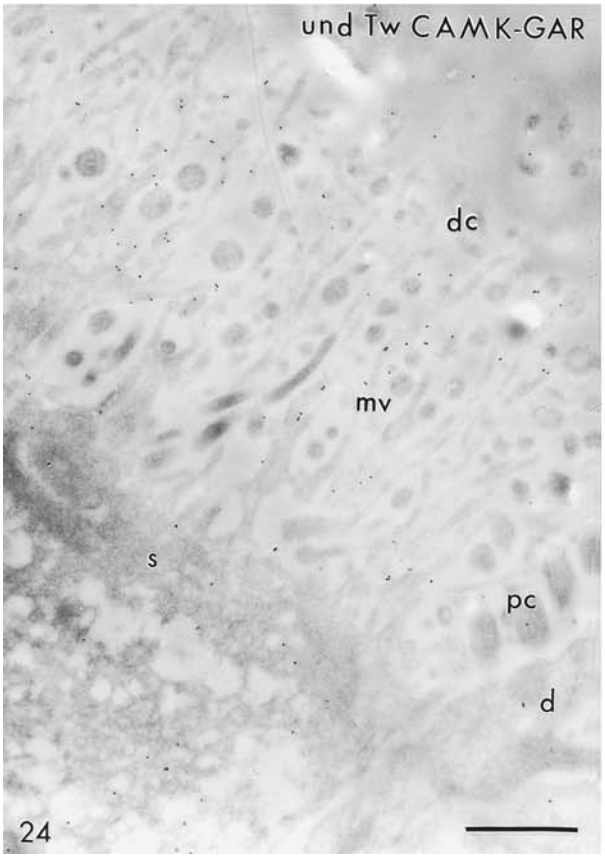
und Tw CAMK-GAR
dc
mv
s
pc
d
24

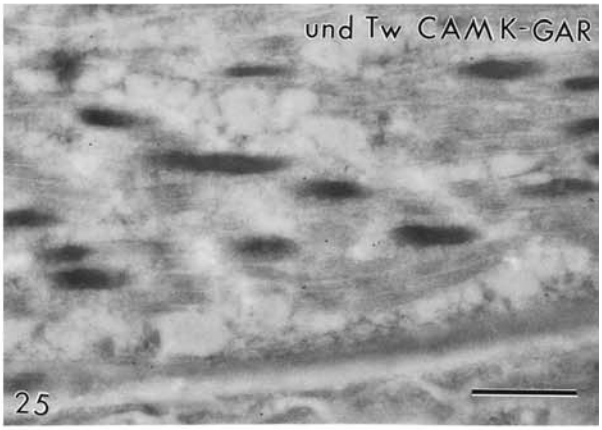
und Tw CAMK-GAR
25

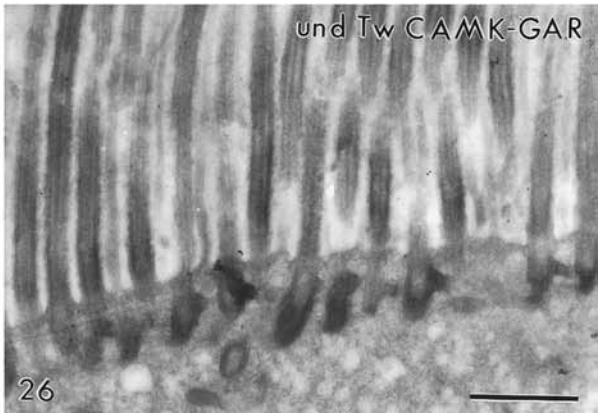
und Tw CAMK-GAR
26

β-arrestin-2, CaMKII and PDE1C2) as seen with electron microscopy were essentially consistent with those seen with light microscopy (Table 1; the light microscopic studies did not include the VNO). In all cases, olfactory epithelial surfaces were labeled and immunoreactivity was present in olfactory cilia. Previous fine-structural studies demonstrated that the distal parts of these cilia are the subcellular structures where the sites of signal onset (Moon & Ronnett, 2003) are concentrated (reviewed in Menco 1997; Menco & Morrison, 2003; also Schwarzenbacher *et al*., 2005). The same was true for microvilli of sensory cells in the VNO; antibodies to molecules of signal-onset solely labeled these structures (Liman *et al*., 1999; Menco *et al*., 2001; Takami, 2002).

In contrast, none of the antibodies to molecules conceivably involved in olfactory signal-termination and -regulation used here labeled olfactory receptor-cell cilia, or other parts of these cells, exclusively. Areas of immunoreactivity included apical structures—microvilli and sometimes apices below them—of supporting cells and, in one case (NKCC1), cytoplasmic compartments of both olfactory epithelial supporting and receptor cells. Except for those to NKCC1 (Table 3), none of the antibodies immunoreacted with VNO receptor cell structures, though apices and microvilli of VNO supporting cells did notably immunoreact with an antibody to CaMKII and one to β-arrestin-2. Labeling of microvilli and apices of smaller populations of microvillous cells, which are different from supporting cells (Carr *et al*., 1995; Morrison & Menco, 2003), of the nasal respiratory epithelium adjacent to the olfactory epithelium and of the morphologically similar VNO non-sensory areas was low or non-existent (Table 3).

The possibility that at least some of the antibodies were not sufficiently specific and, therefore, that labeling of supporting-cell structures is a non-specific phenomenon cannot be completely dismissed. However, there are several arguments against this. First, for all but one (NKCC1) antigens antibodies included those used in earlier light- microscopic investigations, where non-specificity was not noted (Dawson *et al*., 1993; Juilfs *et al*., 1997; Wei *et al*., 1998). Second, where possible we conducted preabsorption controls with antigenic peptides. Though this procedure did not abolish labeling, this gave an overall reduction in labeling compared to conditions where peptide was not included. Third, in all cases, we used more than one antibody against the same protein, and when labeling did occur immunoreactivity patterns for the different antibodies resembled one another (Table 3). Fourth, labeling in the epithelial surfaces was not homogeneous. In all instances, microvilli and apices of microvillous cells that are not supporting cells labeled with a lower efficacy than those of supporting cells (summarized in Table 3). Considering these four arguments, labeling of supporting-cell structures most likely reflects a genuine property of these cells.

A partial explanation for the fact that besides structures of olfactory receptor cells also those of supporting cells immunoreacted with the antibodies to molecules of signal-termination and—regulation may be found in reports that suggest that both cell types as well as, at least to some extent, nasal respiratory epithelial cells have a common origin (Beites *et al*., 2005; Carter *et al*., 2004; Chen *et al*., 2004; Manglapus *et al*., 2004; Murray *et al*., 2003). Distinctions in onset molecules conceivably suffice to differentiate signal processing of olfactory receptor cells from still enigmatic onset cascades in

Fig. 27. Section through rat VNO sensory epithelium prepared in the same way as the olfactory tissues, incubated with the polyclonal antibody to CaMKII α/β, at a dilution of 1:10, without Tween 20 incorporation (as Fig. 22). Apices (s) and microvilli (ms) of supporting cells labeled abundantly, while immunoreactivity was absent from receptor-cell dendrites (d) and microvilli (mr; compare with Fig. 20 where the VNO displayed a similar pattern of labeling). Scale bar = 1 μm.

Fig. 28. Section through rat VNO receptor cell axons exposed to the same CaMKII α/β antibody and conditions as used for the sections of Figs. 22 and 27. Labeling was absent (compare with Figs. 25 and 31). Scale bar = 1 μm.

Fig. 29. Section through rat VNO non-sensory epithelium, prepared in the same way as the olfactory tissues (see legend Fig. 22), where cilia (c) and microvilli (m) were devoid of labeling (compare with Fig. 21). Scale bar = 1 μm.

Fig. 30. Section through the surface of rat olfactory epithelial tissue prepared as described in the legend of Fig. 22, but incubated with a monoclonal antibody to CaMKII β, diluted 1:5, with GAM as the gold (15 nm)-conjugated secondary probe (CAMK-GAM; Line 11 in Table 1). The primary antibody came from the same source as that used in an earlier, light-microscopic, study (Wei *et al*., 1998) on the location of CaMKII in olfactory epithelia. Receptor cell dendritic endings (d), proximal (pc) and distal parts of olfactory cilia (dc), and supporting cell apices (s) and microvilli (mv) are seen labeled (compare with Figs. 22–24). Scale bar = 1 μm.

Fig. 31. Section through rat olfactory receptor cell axons exposed to the same CaMKII β antibody and conditions as used for the section of Fig. 30. There was some axonal labeling, but significantly less than in the surface structures, cilia and microvilli (Fig. 30; compare also with Figs. 25 and 28). Scale bar = 1 μm.

Fig. 32. Section through rat respiratory epithelial surface exposed to the same antibody and conditions as used for the section seen in Fig. 30, but respiratory cilia seen here show lower labeling than the olfactory epithelial surface structures depicted in that figure. Scale bar = 1 μm.

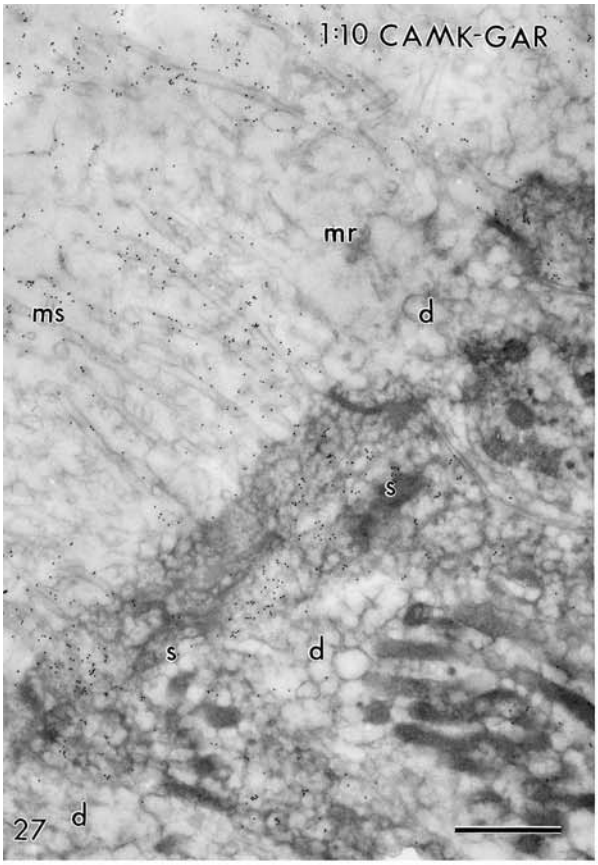
1:10 CAMK-GAR
mr
ms
d
s
s
d
27
d

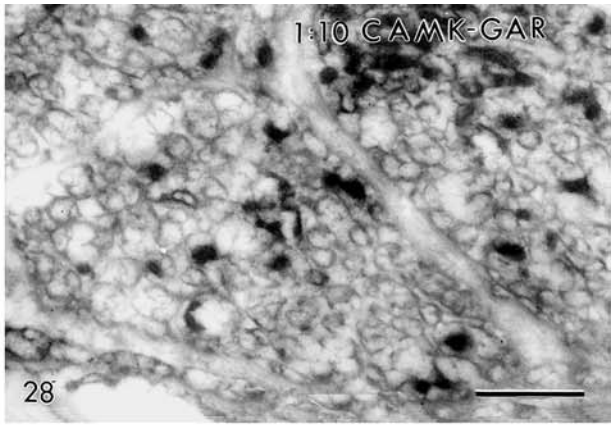
1:10 CAMK-GAR
28

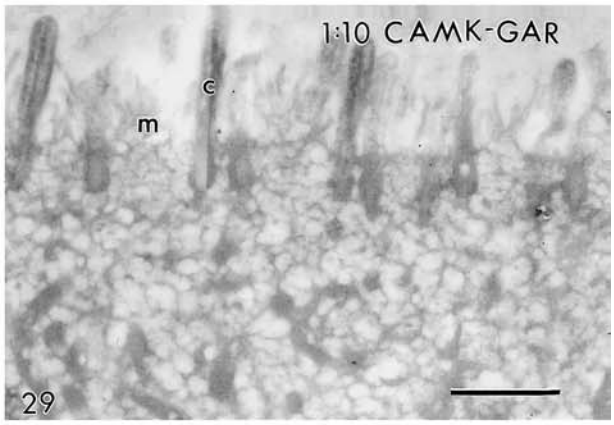
1:10 CAMK-GAR
c
m
29

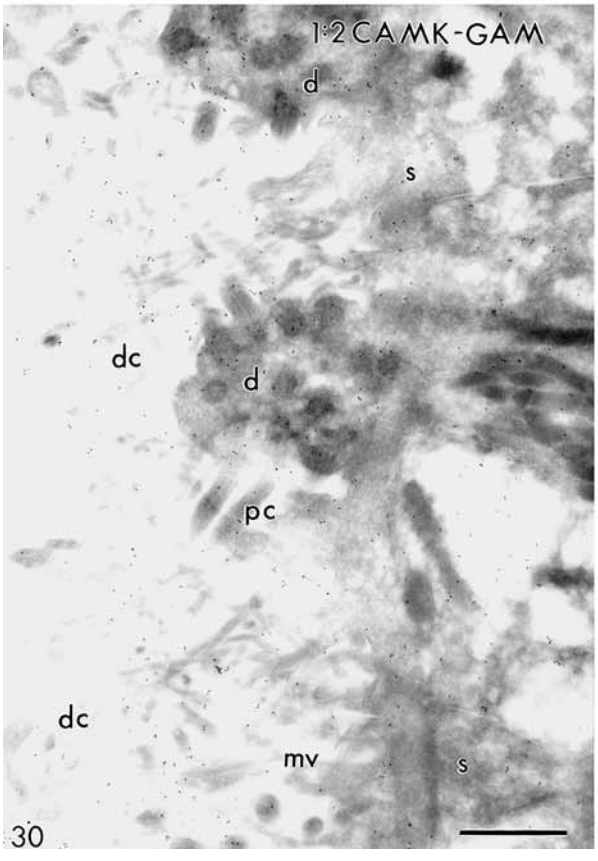
1:2 CAMK-GAM
d
s
dc
d
pc
dc
mv
s
30

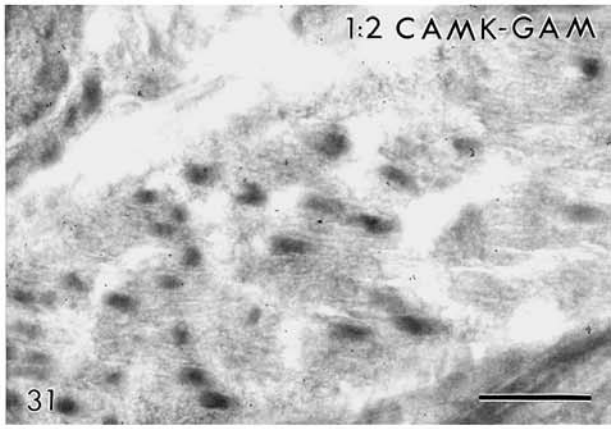
1:2 CAMK-GAM
31

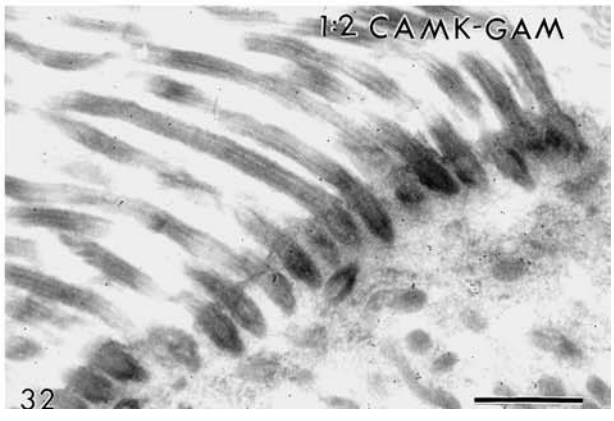
1:2 CAMK-GAM
32

the supporting cells. Consequently differential expression of the molecules investigated here is not necessary, and their presence is a shared property of receptor and neighboring supporting cells. In speculation, supporting cell signaling could reasonably involve odors but other stimuli as well (Carr *et al*., 2001, and references therein). The origin of the various types of microvillous cells that are not typical supporting cells is unknown. Following the above reasoning, the present findings would suggest an origin distinct from that of receptor and supporting cells, e.g., perhaps a special subpopulation of horizontal and/or globose basal cells.

GRK3

GRKs participate in agonist-mediated desensitization by phosphorylating G-protein-coupled receptors (GPCRs) uncoupled from the G-proteins by the GRKs (review, Gainetdinov *et al*., 2003; Table 2). In the mammalian olfactory system, this role is served by GRK3 (Dawson *et al*., 1993; Peppel *et al*., 1997; Schleicher *et al*., 1993). Indeed, this study shows that GRK3 is prominently present in the distal parts of olfactory cilia, the cellular location of olfactory signal-onset (Menco, 1997; Menco & Morrison, 2003).

In neighboring supporting cells, GRK3 likely participates in agonist-mediated desensitization of signaling processes even though these are not yet precisely known. The putative GPCRs of these supporting cells are different from receptor cell odor receptors as there is no evidence that odor receptors are expressed in supporting cells (reviews, Kini & Firestein, 2001; Moon & Ronnett, 2004). In invertebrate chemoreception GRK2 seems to play the same role that GRK3 plays in mammalian olfaction (Fukuto *et al*., 2004). Absence of GRK3 in the VNO suggests that the VNO uses a different signaling cascade, as suggested by many studies (Brennan & Keverne, 2003), including ultrastructural ones (Menco *et al*., 2001; Takami, 2002).

The antibody of Line 1 in Tables 1 and 3 erratically labeled respiratory cilia. This may be due to the heavy labeling of nearby goblet cells that spread out near their mucus vicinities. The antibody common to GRK2 and GRK3 used here labeled dendritic endings and respiratory cilia (Fig. 8; respiratory cilia, not shown; Line 3 in Tables 1 and 3). This antibody is the same as that used in earlier studies (Dawson *et al*., 1993). Some of its labeling, especially in the dendritic endings and respiratory cilia, but also in olfactory cilia, could be due to GRK2 (or β-ARK1). The latter, a kinase associated with microtubules purified from bovine brain, may be involved in β-tubulin phosphorylation (Pitcher *et al*., 1998). Indeed, β-tubulin is amply present in dendrites and sensory and non-sensory cilia (e.g., Figs. 7b in Menco *et al*., 1992, and 5F in Pixley *et al*., 1997). However, since two additional antibodies, both to GRK3 alone, gave a similar

Fig. 33. Section through the surface of rat olfactory epithelial tissue fixed with freshly depolymerized paraformaldehyde and cryoprotected before freeze-substitution. The section was incubated with an antibody to PDE1C2 at a dilution of 1:1,000 with Tween 20 present throughout the whole procedure, and with GAR as the gold (15 nm)-conjugated secondary probe (Tw PDE1-GAR; Line 14 in Table 1). The primary antibody was the same as that used in an earlier, light-microscopic, study on the location of PDE1C2 in olfactory epithelia (Juilfs *et al*., 1997). Distal (dc, small arrow) and proximal segments of olfactory cilia (pc, small asterisks) as well as supporting cell microvilli (mv) are seen labeled. Deeper in the tissue labeling is absent in both the apices of supporting cells (s, large asterisk) and in the receptor cell dendrites (d). Scale bar = 1 μm.

Fig. 34. Section through the surface of rat olfactory epithelial tissue both prepared and exposed to the same antibody as described in the legend of Fig. 33, but at a dilution of 1:100 with GAR-FAB as the gold (15 nm)-conjugated secondary probe (Tw PDE1-FAB). At this higher concentration, dendritic endings (d) of olfactory receptor cells, proximal (pc) and distal parts of their cilia (dc), and supporting cell microvilli (mv) labeled well. Labeling in the supporting cell apices (s) is sparse. Scale bar = 1 μm.

Fig. 35. Section through the surface of rat olfactory epithelial tissue prepared as described in the legend of Fig. 33 and exposed to the same PDE1C2 antibody as used for that figure, but at a dilution of 1:1000 with GAR-FAB-gold (15 nm) as secondary probe. The labeling pattern was the same as that seen in Figs. 33 and 34, which implies that GAR-FAB and GAR worked equally well (GAR-FAB was mostly used in the localization of PDE1C2, hence the comparison). d = Dendritic ending, pc = proximal parts of olfactory cilia, dc = distal parts of olfactory cilia, s = supporting cell apex, mv = supporting cell microvilli. Scale bar = 1 μm.

Fig. 36. Section through rat olfactory receptor cell axons exposed to the same PDE1C2 antibody and conditions as used for the section of Fig. 35. Labeling was absent. Scale bar = 1 μm.

Fig. 37. Section through rat respiratory epithelial surface exposed to the same PDE1C2 antibody and conditions as used for the section seen in Fig. 35. Labeling of respiratory cilia was sparse. Scale bar = 1 μm.

Fig. 38. Section through the surface of rat olfactory epithelial tissue prepared as described in the legend of Fig. 33, but with an antibody to PDE1C2 generated in a different rabbit than the antibody used in Figs. 33–37. This antibody was used at a dilution of 1:10,000, with GAR as the gold (15 nm)-conjugated secondary probe (PDE2-GAR). Microvilli (miv) of a microvillous cell Type II (mi) displayed less labeling than either those of a nearby supporting cell (mv) and its apex (s) (arrowheads) or those of a nearby receptor cell dendritic ending (d) and its cilia (pc). Deeper inside the epithelium labeling was absent from all three cell types (asterisks), which is consistent with the pattern seen in Figure 36, at the level of receptor cell axons. Scale bar = 1 μm.

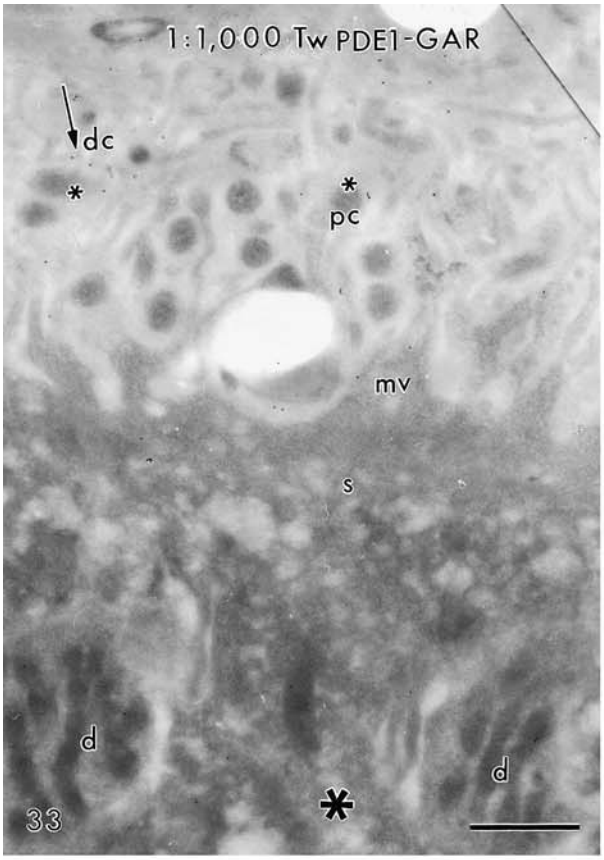
1:1,000 Tw PDE1-GAR
dc
pc
mv
s
d
d
33

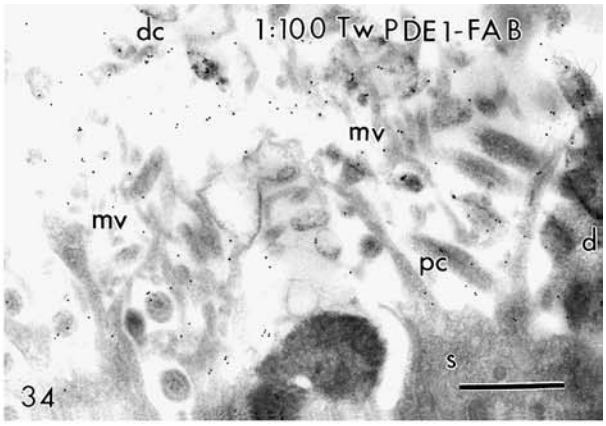
dc
1:100 Tw PDE1-FAB
mv
mv
pc
d
s
34

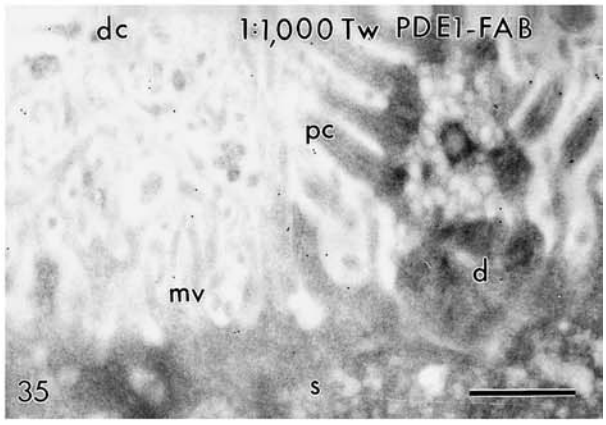
dc
1:1,000 Tw PDE1-FAB
pc
d
mv
s
35

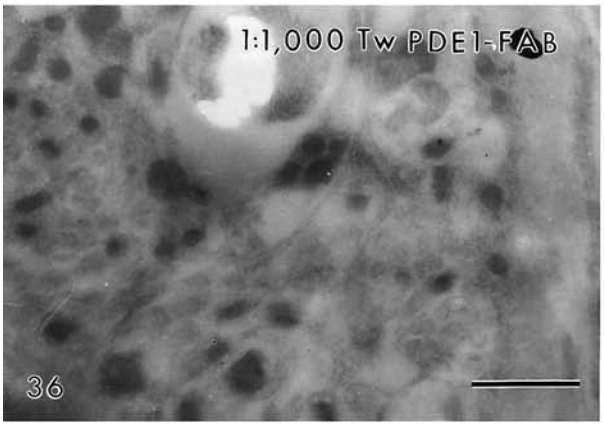
1:1,000 Tw PDE1-FAB
36

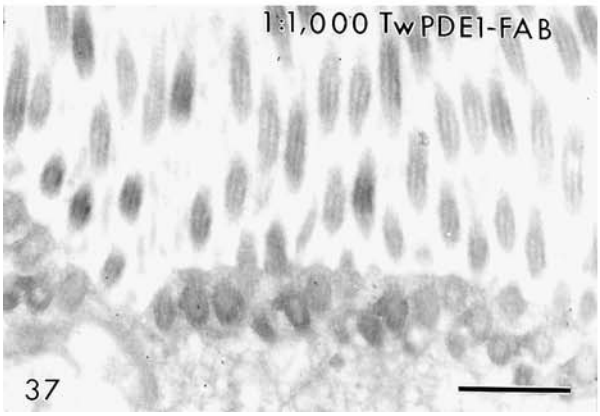
1:1,000 Tw PDE1-FAB
37

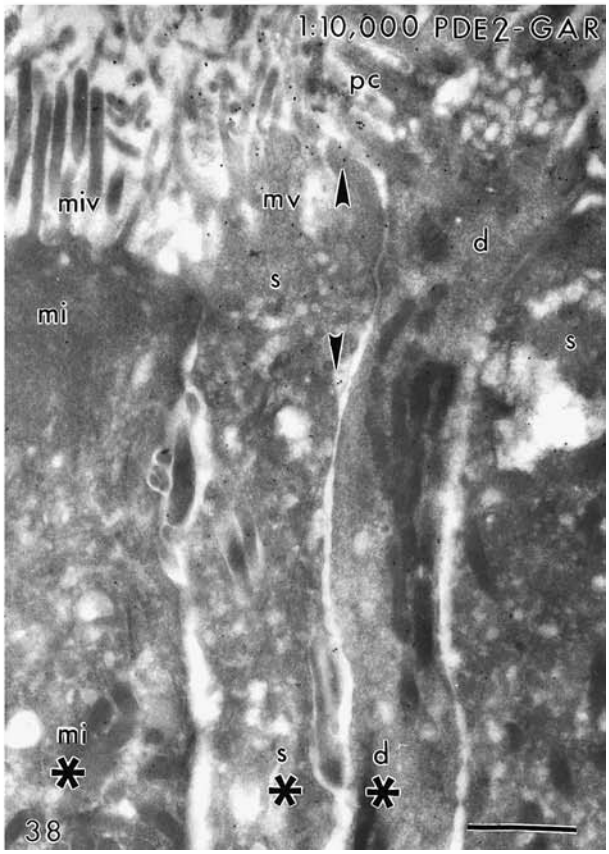
1:10,000 PDE2-GAR
pc
miv
mv
d
s
mi
s
mi
s
d
38

pattern of labeling, the supposition that GRK3 is involved in receptor cell signaling (Boekhoff *et al*., 1994; Bruch *et al*., 1997; Dawson *et al*., 1993; Peppel *et al*., 1997; Schleicher *et al*., 1993) is validated at the level of fine structure.

β-ARRESTIN-2

Following uncoupling of GPCRs from G-proteins by GRKs, phosphorylated GPCRs bind to arrestins, preventing them from further stimulation by G-proteins (Gainetdinov *et al*., 2004). In the vertebrate olfactory system, β-arrestin-2 cooperates with GRK3 in the agonist-mediated desensitization of GPCR-involved signaling processes (Dawson *et al*., 1993; Moon & Ronnett, 2003). The current study shows that the cellular locations of GRK3 and β-arrestin-2 overlap, indeed. This is true not only in receptor cells but also in neighboring supporting cells. Thus, it appears that olfactory receptor and supporting cells use, in addition to the same GRK, the same arrestin in supporting cells for onset cascades that are still obscure. In the VNO, supporting cells labeled throughout their apices with at least one of the antibodies, suggesting that β-arrestin-2 may serve a role here too, though unlikely in association with GRK3 (see Table 3). Indeed, recent studies have shown that β-arrestin-2 and also β-arrestin-1 subserve many cellular functions (reviewed by Lefkowitz & Shenoy, 2005), therefore the ubiquitous presence of this protein in sensory as well as supporting olfactory epithelial cells is not surprising.

CAMKII

CaMKII negatively regulates ACIII by reducing cAMP production, thus decreasing the overall gain in olfactory signaling (Zufall & Leinders-Zufall, 2000; Wei *et al*., 1998). Two out of five antibodies used here gave a positive immunoreactivity for CaMKII. One of these was the same as that used in an earlier study at the light-microscopic level (Wei *et al*., 1998); the Wei study did not specify which of two available Zymed antibodies was used, but only the one to CaMKII β worked presently. The other antibody that worked well was generated to a peptide common to CaMKII α and CaMKII β (Table 1). CaMKII α is involved in the development of olfactory systems in the rodent (Zou *et al*., 2002) and in the chick (Lalloué *et al*., 2003). The present study suggests that CaMKII β is the predominant CaMKII involved in olfactory signaling, at least in rodents. However, once again the results demonstrate that receptor and supporting cells share parts of signaling cascades. In addition, the

---

Fig. 39. Section through the surface of rat olfactory epithelial tissue fixed with freshly depolymerized paraformaldehyde and cryoprotected before freeze-substitution, immunoreacted with the T4 monoclonal antibody to NKCC1/2 Na^+, K^+, Cl^--cotransporter. The antibody was used at a dilution of 1:2, with GAM as the gold (15 nm)-conjugated secondary probe (NKCC-GAM; Line 16 in Table 1). The primary antibody was the same as that used for light-microscopy on the location of NKCC1/2 in olfactory epithelia (see Table 1, legend, note 4). Supporting cell cytoplasmic areas (s) and their microvilli (mv), proximal (pc) and distal parts of olfactory cilia (dc), and the dendrites (d) from which these cilia originate are seen labeled. Scale bar = 1 μm.

Fig. 40. The same area as that seen in Figure 39, but near the nucleus (n) of a supporting cell (s). The cytoplasmic area surrounding the nucleus labeled, but immunoreactivity was absent from the nucleus itself. The border between cytoplasm and nucleus is marked with arrowheads. Scale bar = 1 μm.

Fig. 41. The same area as that seen in Figure 39, but near the nucleus (n) of a receptor cell (d). The cytoplasmic area surrounding the nucleus labeled, though less so than a comparable location in supporting cells (Fig. 40). Labeling was absent from the nucleus itself (below arrowheads). Scale bar = 1 μm.

Fig. 42. Section through rat olfactory receptor cell axons exposed to the same NKCC1/2 antibody and conditions as used in the section of Fig. 39. The intensity of labeling is similar to that seen in the cytoplasmic area of Fig. 41 (above arrowheads). Scale bar = 1 μm.

Fig. 43. Section through rat respiratory epithelial surface exposed to the same NKCC1/2 antibody and conditions as used for the section seen in Fig. 39. Respiratory cilia immunoreacted with the antibody (compare with Fig. 39). Scale bar = 1 μm.

Fig. 44. The same area as that seen in Fig. 43, but near the nucleus (n) of a respiratory cell. As in the olfactory epithelium (Figs. 39–41), the cytoplasmic area surrounding the nucleus (n) labeled, but immunoreactivity was absent from the nucleus itself. The border between cytoplasm and nucleus is marked with arrowheads Scale bar = 1 μm.

Fig. 45. Section through the surface of rat olfactory epithelial tissue prepared as described in the legend of Fig. 39, but immunoreacted with the T4 monoclonal antibody to NKCC1/2 at a dilution of 1:3. In contrast to apex and microvilli (mv) of a nearby supporting cell (s, see Fig. 39), apex (mi) and microvilli of a microvillous (miv) cell Type II displayed little labeling. Scale bar = 1 μm.

Fig. 46. Section through the surface of rat olfactory epithelial tissue prepared as described in the legend of Fig. 39 but incubated with supernatant NS-1 (dilution 1:3) not containing the NKCC1/2 antibodies. No labeling was encountered in this control. pc = Proximal parts of olfactory cilia, mv = supporting cell microvilli, mi = apex microvillous cell, miv = microvilli microvillous cell. Scale bar = 1 μm.

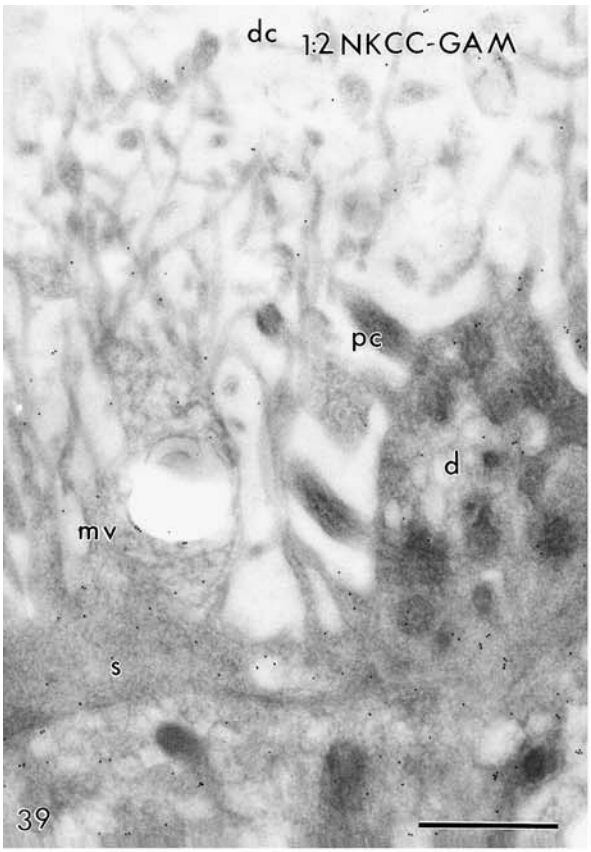
dc
1:2 NKCC-GAM
pc
d
mv
s
39

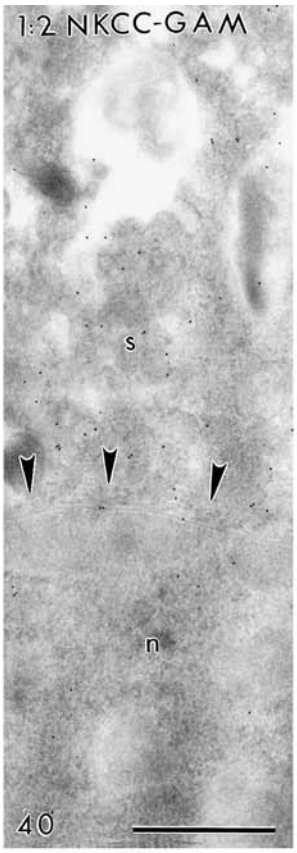
1:2 NKCC-GAM
s
n
40

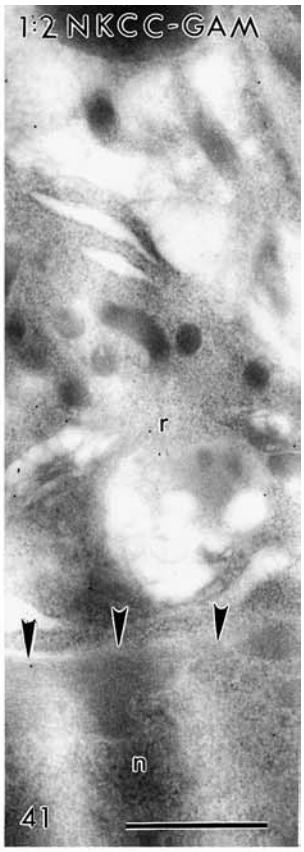
1:2 NKCC-GAM
r
n
41

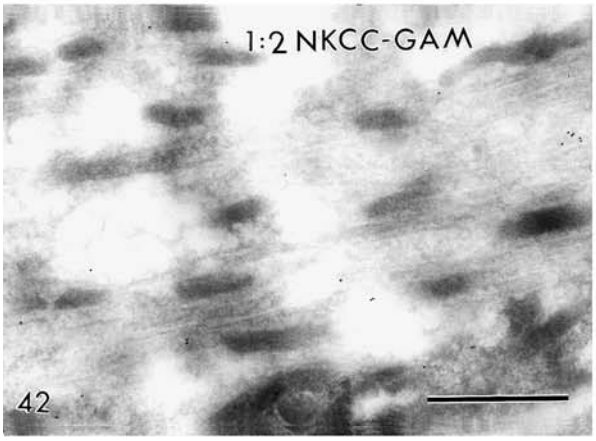
1:2 NKCC-GAM
42

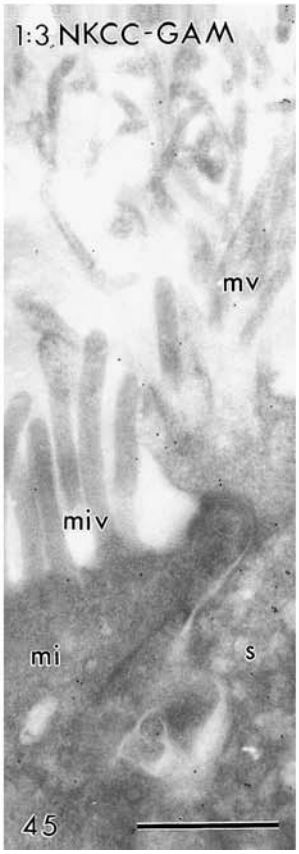
1:3 NKCC-GAM
mv
miv
mi
s
45

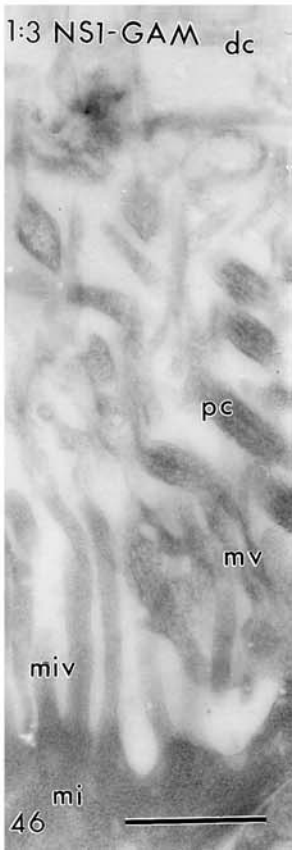
1:3 NS1-GAM
dc
pc
mv
miv
mi
46


1:2 NKCC-GAM
43

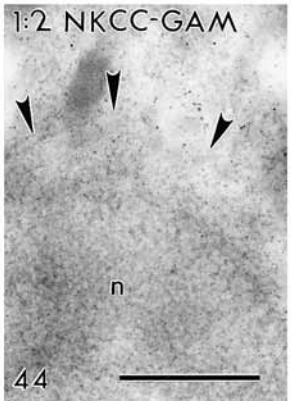
1:2 NKCC-GAM
n
44

results imply that CaMKII has a prominent role in VNO supporting cells, but not, or at least less so, in VNO receptor cells, as these remained unstained.

PDE1C2

Ca^{2+}-calmodulin activates PDE1C2, which in turn stimulates cAMP (and cGMP) hydrolysis. Thus, like CaMKII, PDE1C2 regulates ACIII by reducing cAMP availability (Juilfs *et al*., 1997; Zufall & Leinders-Zufall, 2000). Using the same antibodies as those employed here, light microscopy showed a more prominent labeling of olfactory cilia and dendritic endings that precisely overlapped with ACIII immunoreactivity (Fig. 6A–C in Juilfs *et al*., 1997). Indeed, our data show that the distal parts of olfactory cilia, which contain most of the ACIII (Menco *et al*., 1992, 1994), labeled well. However, supporting cell apical structures, including microvilli, also labeled. An elegant cytochemical study on the fine-structural localization of PDEs in the olfactory epithelium demonstrated that, besides an intense staining of receptor cell cilia, supporting cell microvilli stained faintly (Asanuma & Nomura, 1993). The latter is consistent with a faint residual expression of PDE1C2 mRNA following bulbectomy (Yan *et al*., 1995) and with the present results. The reason for the difference in labeling patterns of the current fine-structural investigations when compared with the light-microscopic work may be antibody promiscuity. We encountered similar, though opposite, differences in earlier studies, e.g., an antibody to a mouse odor receptor was seen to label olfactory receptor cells throughout with light microscopy, whereas fine structural immunoreactivity was restricted to receptor cell cilia (Menco *et al*., 1997).

Although a PDE1C isoform most likely plays a role in VNO signaling (Cherry & Pho, 2002), the present results suggest either that this is not PDE1C2 or that expression of PDE1C2 in the VNO is below the level of sensitivity using the methods employed here. Similarly, in other studies we failed to distinctly localize OMP to VNO receptor cells with immunogold labeling, perhaps caused by the fact that OMP is expressed at a lower level in these cells than in the receptor cells of the main olfactory organ (unpublished and Dr. Frank Margolis, Personal Communication).

NKCC1

A Ca^{2+}-activated chloride channel contributes a high-gain and low-noise amplification to olfactory receptor cell depolarization (Frings *et al*., 2001, Menini, 1999). The Cl^--cotransporters NKCC1 (Lytle *et al*., 1995) and KCC2 (Williams *et al*., 1999) regulate the internal chloride concentration in cells. It is hypothesized that receptor cells that depolarize in response to odors maintain their internal Cl^--levels with NKCC1 (Reisert *et al*., 2005), whereas KCC2 is putatively present in receptor cells that hyperpolarize (Shannen & Delay, 2004). However, only NKCC1-mediated Cl^--uptake was noted in olfactory receptor cells (and supporting cells) and there is no evidence for KCC2 (or for NKCC2) in olfactory epithelia (Kaneko *et al*., 2004; Reisert *et al*., 2005). Fine-structural localization of these molecules was included in this study. Indeed, we did not find immunoreactivity for an antibody to KCC2 (Williams *et al*., 1999). Regarding cell bodies and dendrites our findings in receptor cells are in line with those of Reisert *et al*. (2005), but we found that the cotransporter is also present in dendritic knobs and cilia and seemingly axons. The studies of Kaneko *et al*. (2004) and Reisert *et al*. (2005) suggest that the function of NKCC1 in receptor cells is to maintain the receptor cell intracellular Cl^--concentration above electrochemical equilibrium (see also Restrepo, 2005).

The present study also showed that the cotransporter was more abundant in supporting cells than in receptor cells, where it was similarly expressed throughout the cells. The same can be seen in Fig. 2B of Reisert *et al*. (2005), although they ascribed that labeling to a subpopulation of supporting cells, possibly microvillous cells. However, this study showed that "regular" supporting cells rather than microvillous cells contain most of the label. The fact that supporting cells labeled more intensely in corresponding cellular regions than receptor cells suggests that these supporting cells require relatively more of this cotransporter than olfactory receptor cells. In supporting cells the cotransporter may play an important role in controlling Cl^- in the environment of the receptor cells. A need for NKCC1 in supporting cells is shared with other transporting cells where NKCC1 is found in basolateral membranes, in particular cells of kidney collecting tubules (Wall & Fisher, 2002), but also of cells that

Fig. 47. Section through the surface of rat olfactory epithelial tissue prepared as described in the legend of Fig. 39, immunoreacted with the T4 monoclonal antibody to NKCC1/2 at a dilution of 1:2 (like Figs. 39–44). Here it can be better seen that, in contrast to apex (*s*) and microvilli (mv) of a nearby supporting cell, apex (mi) and microvilli of a microvillous cell (miv) Type II displayed little labeling for the antibody to NKCC1/2. pc = Proximal parts of olfactory cilia. Scale bar=1 μm.

Fig. 48. Section through the surface of rat olfactory epithelial tissue fixed with freshly depolymerized paraformaldehyde and cryoprotected before freeze-substitution, GAR control. Labeling was absent in all structures. d = Dendritic ending, pc = proximal parts of olfactory cilia, dc=distal parts of olfactory cilia, s = supporting cell apex, mv = supporting cell microvilli. Scale bar = 1 μm.

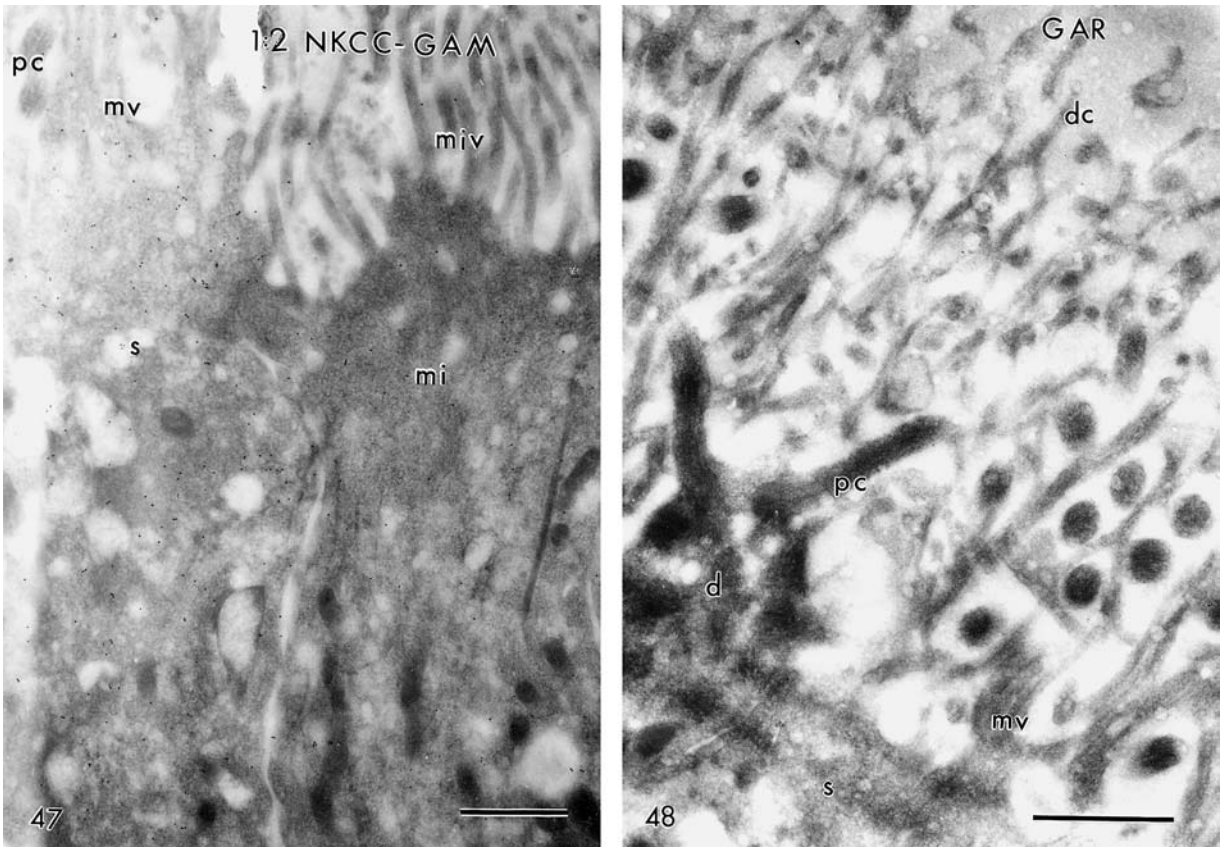

maintain the endolymph in cochlea (Sakaguchi *et al*., 1998). The present result is in line with earlier findings on the putative role of supporting cells in the maintenance of the olfactory receptor cell environment. These showed that supporting cell microvilli, again like apical regions of principal cells of kidney collecting tubules, contain an abundance of amiloride-sensitive but voltage-insensitive Na^+-channels, suggesting that these cells are involved in Na^+-reabsorption (Menco *et al*., 1998; Menco & Morrison, 2003). In any case, from this work it appears that a role for NKCC1 in olfactory epithelia likely involves more than receptor cells alone.

NKCCs are transmembrane proteins (Gagnon *et al*., 2004). Here, however, NKCC1 was distributed throughout labeled cells, apart from nuclei, and the same appears to be true with light microscopy (Fig. 2B in Reisert *et al*., 2005). This may mean that the antibody also labeled precursor and/or breakdown products of NKCC1 during trafficking in addition to its final membrane product. Absence of NKCC1 in the VNO suggests that in this system receptor and supporting cells likely make use of different cotransporters.

ADDITIONAL MOLECULES OF OLFACTORY SIGNALING THAT NEED FINE STRUCTURAL EVALUATION

The list of proteins thought to be involved in olfactory signal-termination and -regulation is not exhausted with those studied here (Morrison & Menco, 2003; Yu *et al*., 2005). Calmodulin is thought to play a pivotal role in olfactory desensitization at various levels (reviewed by Menini, 1999; Moon & Ronnett, 2003; Zufall & Leinders-Zufall, 2000), even under native conditions (Bradley *et al*., 2004). However, light microscopy, though showing that calmodulin is present in cell bodies, did not demonstrate its presence in receptor cell cilia (Bastianelli *et al*., 1995), implying a need for additional ultrastructural studies. Similarly, regulators of G-protein signaling (RGSs) influence signal termination by inhibiting ACIII (Bruch & Medler, 1996; Sinnaraja *et al*., 2001), but the fine-structural location of these proteins has not yet been shown.

Conclusion

The observations suggest that none of the molecules that are supposedly involved in olfactory signal-termination and -modulation (GRK3, β-arrestin-2, CAMKII, PDE1C2, and NKCC1) and that are investigated here for their fine-structural localization in olfactory epithelia are precisely and exclusively located in the same subcellular regions as molecules of olfactory signal-onset, that is olfactory cilia (Menco, 1997; Menco & Morrison, 2003). Rather, olfactory receptor cells and neighboring supporting cells and, in part VNO supporting cells share these molecules of signal transduction. In regard to the receptor cells of the main olfactory organ, it is interesting to note that recent

electrophysiological work (Bhandawat *et al*., 2005) has suggested that termination of the activity of the odorant receptor may involve simply the unbinding of the odorant rather than phosphorylation of the receptor and subsequent binding by β-arrestin-2. These authors suggest that desensitization by phosphorylation in olfactory signaling may only be important upon prolonged and intense stimulation. In that case, supporting cells of the main olfactory organ are also affected (Carr *et al*., 2001, and references therein). In these supporting cells, molecules of desensitization occur in addition to those of biotransformation and transepithelial transport (Carr *et al*., 2001; Menco *et al*., 1998; Yu *et al*., 2005; review, Menco & Morrison, 2003).

Acknowledgments

The author thanks Drs. J. A. Beavo (Department of Pharmacology, University of Washington, Seattle, WA) and R. J. Lefkowitz (Howard Hughes Medical Institute, Duke University Medical Center, Durham, NC) for the generous donation of antibodies to PDE1C2 and the A2CT antibody to β-arrestin-2, respectively. The critical review of Drs. N. K. Kleene, S. J. Kleene (Department of Cell Biology, Neurobiology, and Anatomy, University of Cincinnati, Cincinnati, OH) and anonymous reviewers in the preparation of this manuscript was very much appreciated. Drs. N. K. and S. J. Kleene are also thanked for inciting the work on Cl^--cotransporters and for help in obtaining the T4 and B22pAB antibodies and appropriate controls. The donation of anti-OMP and anti-$G_{olf\alpha}$ used as controls by Drs. F. L. Margolis (Department of Anatomy, University of Maryland School of Medicine, Baltimore, MD) was greatly appreciated. Danielle N. Lodwyck (Northwestern University Department of Communication Sciences and Disorders) is thanked for the work on the NKCC1 polyclonal antibody (Line 18 in Table 1). The help of Mickie Weiss in the editing of the manuscript of this work was greatly appreciated. This material is based upon work supported by the National Science Foundation under Grant No. 0094709.

Note added in proof

The fact that olfactory epithelial sensory and supporting cells share several proteins, as found here, thought to be specific for receptor cells (or more general, for neurons) extends to several proteins thought to be neuron-specific (forthcoming articles in these series: Maroldt *et al*., 2005: Weiler & Benali, 2005). This reinforces the notion of a common origin of both cells (see Discussion, first part).

References

ASANUMA, N. & NOMURA, H. (1993) Cytochemical localization of cyclic 3′,5′-nucleotide phosphodiesterase activity in the rat olfactory receptor mucosa. *Histochemical Journal* **25**, 348–356.

BASTIANELLI, E., POLANS, A. S., HIDAKA, H. & POCHET, R. (1995) Differential distribution of six calcium-binding proteins in the rat olfactory epithelium during postnatal development and into adulthood. *The Journal of Comparative Neurology* **354**, 395–409.

BEITES, C. L., KAWAUCHI, S., CROCKER, C. E. & CALOF, A. L. (2005) Identification and molecular regulation of neural stem cells in the olfactory epithelium. *Experimental Cell Research* **306**, 309–316.

BHANDAWAT, V., REISERT, J. & YAU, K.-W. (2005) Elementary response of olfactory receptor neurons to odorants. *Science* **308**, 1931–1934.

BOEKHOFF, I., INGLESE, J., SCHLEICHER, S., KOCH, W. J., LEFKOWITZ, R. J. & BREER, H. (1994) Olfactory desensitization requires membrane targeting of receptor kinase mediated by $\beta\gamma$-subunits of heterotrimeric G proteins. *The Journal of Biological Chemistry* **269**, 37–40.

BORISY, F. F., RONNETT, G. V., CUNNINGHAM, A. M., JUILFS, D., BEAVO, J. & SNYDER, S. H. (1992) Calcium/calmodulin-activated phosphodiesterase expressed in olfactory receptor neurons. *The Journal of Neuroscience* **12**, 915–923.

BRADLEY, J., BÖNIGK, W., YAU, L.-W. & FRINGS, S. (2004) Calmodulin permanently associates with rat olfactory CNG channels under native conditions. *Nature Neuroscience* **7**, 705–710.

BRENNAN, P. A. & KEVERNE, E. B. (2003) The vomeronasal organ. In *Handbook of Olfaction and Gustation, 2*nd *edition*(edited by DOTY, R. L.), pp. 967–979. New York, NY: Marcel Dekker, Inc.

BRUCH, R. C., KANG, J., MOORE, M. L., JR. & MEDLER, K. F. (1997) Protein kinase C and receptor kinase gene expression in olfactory receptor neurons. *Journal of Neurobiology* **33**, 387–394.

BRUCH, R. C. & MEDLER, K. F. (1996) A regulator of G-protein signaling in olfactory receptor neurons. *NeuroReport* **7**, 2941–2944,

CARR, V. McM., FARBMAN, A. I., COLETTI, L. M. & MORGAN, J. I. (1991) Identification of a new nonneuronal cell type in rat olfactory epithelium. *Neuroscience* **45**, 433–449.

CARR, V. McM., MENCO, B. Ph. M., YANKOVA, M. P., MORIMOTO, R. I. & FARBMAN, A. I. (2001) Odorants as cell-type specific activators of a heat shock response in the rat olfactory mucosa. *The Journal of Comparative Neurology* **432**, 425–439.

CARTER, L. A., MACDONALD, J. L. & ROSKAMS, J. A. (2004) Olfactory horizontal basal cells demonstrate a conserved multipotent progenitor phenotype. *The Journal of Neuroscience* **24**, 5670–5683.

CHEN, X., FANG, H. & SCHWOB, J. E. (2004) Multipotency of purified, transplanted globose basal cells in olfactory epithelium. *The Journal of Comparative Neurology* **469**, 457–474.

CHERRY, J. A. & PHO, V. (2002) Characterization of cAMP degradation by phosphodiesterase in the accessory olfactory system. *Chemical Senses* **27**, 643–652.

DAWSON, T. M., ARRIZA, J. L., JAWORSKY, D. E., BORISY, F. F., ATTRAMADAL, H., LEFKOWITZ, R. J. & RONNETT, G. V. (1993) β-Adrenergic

receptor kinase-2 and β-arrestin-2 as mediators of odorant-induced desensitization. *Science* **259**, 825–829.

FRINGS, S. (2001) Chemoelectrical signal transduction in olfactory sensory neurons of air-breathing vertebrates. *Cellular and Molecular Life Sciences* **58**, 510–519.

FRINGS, S., REUTER, D. & KLEENE, S. J. (2000) Neuronal Ca^{2+} -activated Cl^- channels-homing in on an elusive channel species. *Progress in Neurobiology* **60**, 247–289.

FUKUTO, H, S., FERKEY, D. M., APICELLA, A. J., LANS, H., SHARMEEN, T., CHEN, W., LEFKOWITZ, R. J., JANSEN, G., SCHAFER, W. R. & HART, A. C. (2004) G protein-coupled receptor kinase function is essential for chemosensation in *C. elegans*. *Neuron* **42**, 581–593.

GAGNON, E., BERGERON, M. J., BRUNET, G. M., DAIGLE, N. D., SIMARD, S. F. & ISENRING, P. (2004) Molecular mechanisms of Cl^- transport by the renal Na^+-K^+-Cl^- cotransporter. Identification of an intracellular locus that may from part of a high affinity Cl^- binding site. *The Journal of Biological Chemistry* **279**, 5648–5654.

GAINETDINOV, R. R., PREMONT, R. T., BOHN, L. M., LEFKOWITZ, R. J., CARON, M. G. (2004) Desensitization of G-protein-coupled receptors and neuronal functions. *Annual Reviews of Neuroscience* **27**, 107–144.

JUILFS, D. M., FÜLLE, H.-J., ZHAO, A. Z., HOUSLAY, M. D., GARBERS, D. L. & BEAVO, J. A. (1997) A subset of olfactory neurons that selectively express cGMP-stimulated phosphodiesterase (PDE2) and guanylyl cyclase-D define a unique olfactory signal transduction pathway. *Proceedings of the National Academy of Sciences, USA* **94**, 3388–3395.

KANEKO, H., PUTZIER, I., FRINGS, S., KAUPP, U. B. & GENSCH, T. (2004) Chloride accumulation in mammalian olfactory sensory neurons. *The Journal of Neuroscience* **24**, 7931–7938.

KAUPP, U. B. & SEIFERT, R. (2002) Cyclic nucleotide-gated ion channels. *Physiological Reviews* **82**, 769–824.

KINI, A. D. & FIRESTEIN, S. (2001) The molecular basis of olfaction. *Chimia* **55**, 453–459.

KOO, J. H., GILL, S., PANNELL, L. K., MENCO, B. PH. M., MARGOLIS, J. W. & MARGOLIS, F. L. (2004) The interaction of Bex and OMP reveals a dimer of OMP with a short half-life. *Journal of Neurochemistry* **90**, 102–116.

KULAGA, H. M., LEITCH, C. C., EICHERS, E. R., BADANO, J. L., LESEMANNN, A., HOSKINS, B. E., LUPSKI, J. R., BEALES, P. L., REED, R. R. & KATSANIS, N. (2004) Loss of BBS proteins causes anosmia in humans and defects in olfactory cilia structure and function. *Nature Genetics* **36**, 994–998.

LALLOUE, F. L., AYER-LE LIÈVRE, C. S. & SICARD, G. (2003) Analysis of the functional maturation of olfactory neurons in chicks before and after birth. *Chemical Senses* **28**, 729–737.

LEFKOWITZ, R. J. & SHENOY, S. K. (2005) Transduction of receptor signals by β-arrestins. *Science* **308**, 512–517.

LIMAN, E. R., COREY, D. P. & DULAC, C. (1999) Cloning and localization of TRP2, a candidate transduction channel for mammalian pheromone reception. *Proceedings of the National Academy of Sciences, USA* **96**, 5791–5796.

LYTLE, C., XU, J.-C., BIEMESDERFER, D. & FORBUSH III, B. (1995) Distribution and diversity of Na-K-Cl cotransport proteins: a study with monoclonal antibodies. *American Journal of Physiology* **269**, C1496–C1505.

MANGLAPUS, G. L., YOUNGENTOB, S. L. & SCHWOB, J. E. (2004) Expression patterns of basic helix-loop-helix transcription factors define subsets of olfactory progenitor cells. *The Journal of Comparative Neurology* **479**, 216–233.

MAROLDT, H., KAPLINOVSKY, T. & CUNNINGHAM, A. M. (2005) Immunohistochemical expression of two members of the GDNF family of growth factors and their receptors in the olfactory system. *Journal of Neurocytology* **34**, these issues, in preparation.

MATSUZAKI, O., BAKIN, R. E., MENCO, B. PH. M., CAI, X. & RONNETT, G. V. (1999) Immunolocalization of the olfactory cyclic nucleotide-gated channel subunit 1 (OCNC1) in normal and regenerating olfactory neuroepithelium. *Neuroscience* **94**, 131–140.

MENCO, B. PH. M. (1989) Electron microscopic demonstration of olfactory-marker protein with protein G-gold in freeze-substituted, Lowicryl K11M-embedded rat olfactory receptor cells. *Cell and Tissue Research* **256**, 275–281.

MENCO, B. PH. M. (1995) Freeze-fracture, deep-etch, and freeze-substitution studies of olfactory epithelia, with special emphasis on immunocytochemical variables. *Microscopy Research and Technique* **32**, 337–356.

MENCO, B. PH. M. (1997) Ultrastructural aspects of olfactory signaling. *Chemical Senses* **22**, 295–311.

MENCO, B. PH. M. (2004) The fine structural distribution G-protein receptor kinase 3 (GRK3), β-arrestin-2, Ca^{++}/calmodulin-dependent protein kinase II (CAMKII), and phosphodiesterase PDE1C2 in olfactory epithelia. *Proceedings AChemS* **XXVI**, 101, Abstr. 382.

MENCO, B. PH. M., BIRRELL, G. B., FULLER, C. M., EZEH, P. I., KEETON, D. A. & BENOS, D. J. (1998) Ultrastructural localization of amiloride-sensitive sodium channels and Na^+,K^+-ATPase in the rat's olfactory epithelial surface. *Chemical Senses* **23**, 137–149.

MENCO, B. PH. M., BRUCH, R. C., DAU, B. & DANHO, W. (1992) Ultrastructural localization of olfactory transduction components: The G protein subunit $G_{olf\alpha}$ and type III adenylyl cyclase. *Neuron* **8**, 441–453.

MENCO, B. PH. M., CARR, V. MCM., EZEH, P. I., LIMAN, E. R. & YANKOVA, M. P. (2001) Ultrastructural localization of G-proteins and the channel protein TRP2 to microvilli of rat vomeronasal receptor cells. *The Journal of Comparative Neurology* **438**, 468–489.

MENCO, B. PH. M., CUNNINGHAM, A. M., QASBA, P., LEVY, N. & REED, R. R. (1997) Putative odour receptors localize in cilia of olfactory receptor cells in rat and mouse; a freeze-substitution ultrastructural study. *Journal of Neurocytology* **26**, 297–312 & 691–706 (erratum).

MENCO, B. PH. M. & JACKSON, J. E. (1997) Cells resembling hair cells in developing rat olfactory and nasal respiratory epithelia. *Tissue & Cell* **29**, 707–713.

MENCO, B. PH. M. & MORRISON, E. E. (2003) Morphology of the mammalian olfactory epithelium: Form, fine structure, function, and pathology. In *Handbook of Olfaction and Gustation, 2nd edition* (edited by DOTY, R. L.), pp. 17–49. New York, NY: Marcel Dekker, Inc.

MENCO, B. PH. M., TEKULA, F. D., FARBMAN, A. I. & DANHO, W. (1994) Developmental expression of G-proteins and adenylyl cyclase in peripheral olfactory systems. Light microscopic and freeze-substitution electron

microscopic immunocyto chemistry. *Journal of Neurocytology* **23**, 708–727.

MENINI, A. (1999) Calcium signalling and regulation in olfactory neurons. *Current Opinion in Neurobiology* **9**, 419–426.

MOON, C. & RONNET, G. V. (2003) Molecular neurobiology of olfactory transduction. In *Handbook of Olfaction and Gustation, 2nd edition* (edited by DOTY, R. L.), pp. 75–91. New York, NY: Marcel Dekker, Inc.

MORAN, D. T., ROWLEY, J. C., III & JAFEK, B. W. (1982) Electron microscopy of human olfactory epithelium reveals a new cell type: The microvillar cell. *Brain Research* **253**, 39–46.

MURRAY, R. C., NAVI, D., FESENKO, J., LANDER, A. D. & CALOF, A. L. (2003) Widespread defects in the primary olfactory pathway caused by loss of Mash1 function. *The Journal of Neuroscience* **23**, 1769–1780.

NAKAMURA, T. (2000) Cellular and molecular constituents of olfactory sensation in vertebrates. *Comparative Biochemistry and Physiology Part A* **126**, 17–32.

PEPPEL, K., BOEKHOFF, I., MCDONALD, P., BREER, H., CARON, M. G. & LEFKOWITZ, R. J. (1997) G protein-coupled receptor kinase 3 (GRK3) gene disruption leads to loss of odorant receptor desensitization. *The Journal of Biological Chemistry* **41**. 25425–25428.

PHILLIPS, T. E. & BOYNE, A. F. (1984) Liquid-nitrogen bound quick freezing: Experiences with bounce-free delivery of cholinergic nerve-terminals to a metal surface. *Journal of Electron Microscopy Technique* **1**, 9–29.

PITCHER, J. A., HALL, R. A., DAAKA, Y., ZHANG, J., FERGUSON, S. S., HESTER, S., MILLER, S., CARON, M. G., LEFKOWITZ, R. J. & BARAK, L. S. (1998) The G protein-coupled receptor kinase 2 is a microtubule-associated protein kinase that phosphorylates tubulin. *The Journal of Biological Chemistry* **273**, 12316–12324.

PIXLEY, S. K., FARBMAN, A. I. & MENCO, B. PH. M. (1997) A monoclonal antibody marker for olfactory sustentacular cell microvilli. *The Anatomical Record* **248**, 307–321.

REISERT, J., YAU, K. & BRADLEY, J. (2005) Mechanism of the excitatory Cl- response in mouse olfactory receptor neurons. *Neuron* **45**, 553–561.

RESTREPO, D. (2005) The ins and outs of intracellular chloride in olfactory receptor neurons. *Neuron* **45**, 481–482.

SAKAGUCHI, N., CROUCH, J. J., LYTLE, C. & SCHULTE, B. A. (1998) Na-K-Cl cotransporter expression in the developing and senescent gerbil cochlea. *Hearing Research* **118**, 114–122.

SANDS, J. M. (2004) Renal urea transporters. *Current Opinion in Nephrology & Hypertension* **13**, 525–532.

SCHLEICHER, S., BOEKHOFF, I., ARRIZA, J., LEFKOWITZ, R. J. & BREER, H. (1993) A β-adrenergic receptor kinase-like enzyme is involved in olfactory signal termination. *Proceedings of the National Academy of Sciences, USA* **90**, 1420–1424.

SCHWARZENBACHER, K., FLEISCHER, J. & BREER, H. (2005) Formation and maturation of olfactory cilia monitored by odorant receptor-specific antibodies. *Histochemistry and Cell Biology* **123**, 419–428.

SHANNEN, A. P. & DELAY, R. J. (2004) Expression of Cl-cotransporters in mouse olfactory epithelium. *Proceedings AChemS***XXVI**,*Sarasota, FL*, 73, abstract 281.

SINNARAJAH, S., DESSAUER, C. W., SRIKUMAR, D., CHEN, J., YUEN, J., YILMA, S., DENNIS, J. C., MORRISON, E. E., VODYANOY, V. & KEHRL, J. H. (2001) RSG2 regulates signal transduction in olfactory neurons by attenuating activation of adenylyl cyclase III. *Nature* **409**, 1051–1055.

STROTMANN, J., LEVAI, O., FLEISCHER, J., SCHWARZENBACHER, K. & BREER, H. (2004) Olfactory receptor proteins in axonal processes of chemosensory neurons. *The Journal of Neuroscience* **24**, 7754–7761.

TAKAMI, S. (2002) Recent progress in the neurobiology of the vomeronasal organ. *Microscopy Research and Technique* **58**, 228–250.

VAN LOOKEREN CAMPAGNE, M. B., OESTREICHER, B., VANDER KRIFT, T. P., GISPEN, W. H. & VERKLEIJ, A. J. (1991) Freeze-substitution and Lowicryl HM20 embedding of fixed rat brain: Suitability for immunogold ultrastructural localization of neural antigens. *The Journal of Histochemistry and Cytochemistry* **39**, 1267–1279.

WALL, S. M. & FISCHER, M. P. (2002) Contribution of the Na^+-K^+-$2Cl^-$ cotransporter (NKCC1) to transepithelial transport of H^+, $NH4^+$, K^+, and Na^+ in rat outer medullary collecting duct. *Journal of the American Society of Nephrology* **13**, 827–835.

WEI, J., ZHAO, A. Z., CHAN, G. C. K., BAKER, L. P., IMPEY, S., BEAVO, J. A. & STORM, D. R. (1998) Phosphorylation and inhibition of olfactory adenylyl cyclase by CaM kinase II in neurons: A mechanism for attenuation of olfactory signals. *Neuron* **21**, 495–504.

WEILER, E. & BENALI, A. (2005) Neuronal markers in olfactory tissues. *Journal of Neurocytology* **34**, these issues, in preparation.

WILLIAMS, J. R., SHARP, J. W., KUMARI, V. G., WILSON, M. & PAYNE, J. A. (1999) The neuron-specific K-Cl cotransporter, KCC2. *The Journal of Biological Chemistry* **274**, 12656–12664.

YAN, C., ZHAO, A. Z., BENTLEY, J. K., LOUGHNEY, K., FERGUSON, K. & BEAVO, J. A. (1995) Molecular cloning and characterization of a calmodulin-dependent phosphodiesterase enriched in olfactory sensory neurons. *Proceedings of the National Academy of Sciences, USA* **92,** 9677–9681.

ZOU, D.-J., GREER, C. A. & FIRESTEIN, S. (2002) Expression patterns of α CaMKII in the mouse main olfactory bulb. *The Journal of Comparative Neurology* **443**, 226–236.

ZUFALL, F. & LEINDERS-ZUFALL, T. (2000) The cellular and molecular basis of odor adaptation. *Chemical Senses* **25**, 473–481.

YU, T. T., MCINTYRE, J. C., BOSE, S. C., HARDIN, D., OWEN, M. C. & MCCLINTOCK, T. S. (2005) Differentially expressed transcripts from phenotypically identified olfactory sensory neurons. *The Journal of Comparative Neurology* **483**, 251–262.